


Summer Internship Review Presentation

Kurucz Models - Synthetic Spectral Energy Distribution
Generation and Fitting

Under the Guidance of
Dr. Sarita Vig, Associate Professor, Dept. of ESS

By,
Kiran L (SC17B150)

Contents

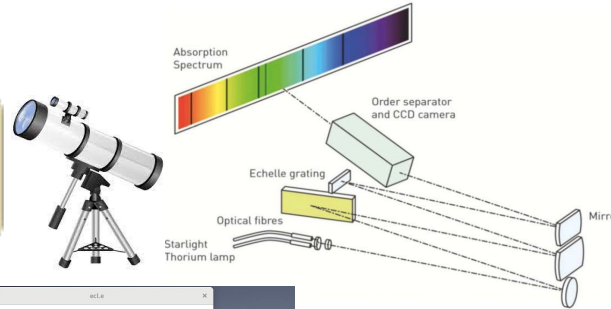
1. Introduction
2. Literature Review
3. Data Description
4. Theory
5. Spectral Energy Distribution Fitting
6. Analysis - Observations and Inferences
7. Conclusion
8. Future Enhancements



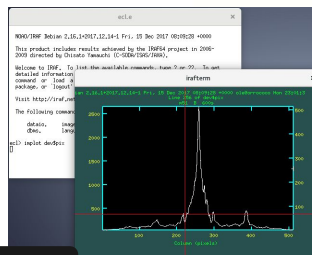
Introduction

Introduction

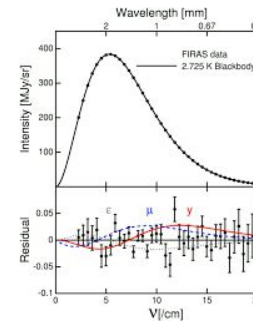
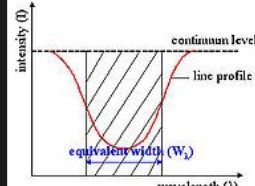
Spectroscopic Observation



Data Reduction



Measurement of stellar parameters



Astrophysical interpretation



1. Spectroscopic determination of properties of stars - method - synthetic spectrum fitting
2. The models are built based on the theory of radiative transfer and stellar spectroscopy.
3. The synthetic spectra find application in determining source properties as well as in population synthesis studies in galaxies.



Literature Review

Literature Review

1. V. Straižys, R. Lazauskaitė and G. Valiauga, 1997.

- a. Compared synthetic energy distributions of the Kurucz models with mean energy distributions of stars of various spectral types (of solar metallicity) - published by Straižys & Sviderskiene (1972)
- b. Model SED found to match mean SED of MS, subgiant and supergiant stars
- c. Considered only visible and near UV portion of observed spectra.
- d. Largest deviation found in UV in early type stars (especially,B-supergiants)
- e. Fit found to be unacceptable for K7-M type stars of all luminosity classes

Literature Review

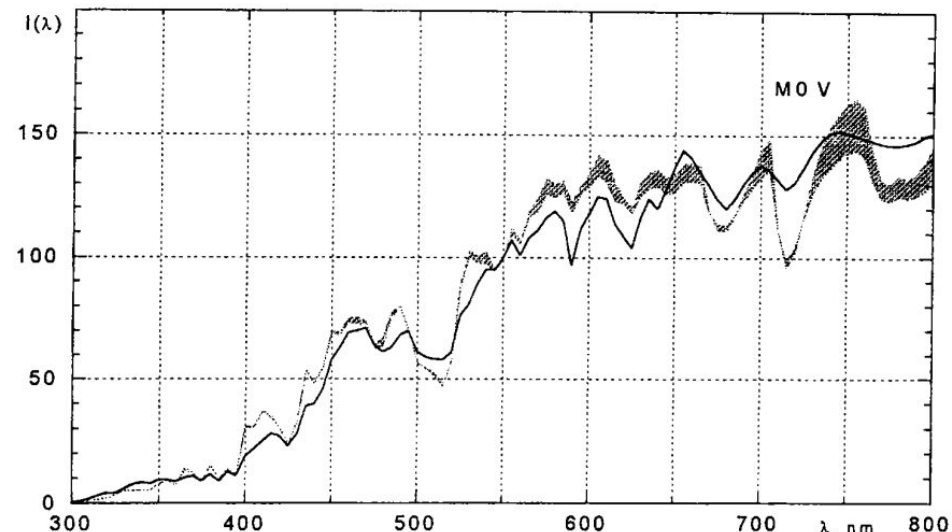


Figure: Un-acceptable fit to M type stars

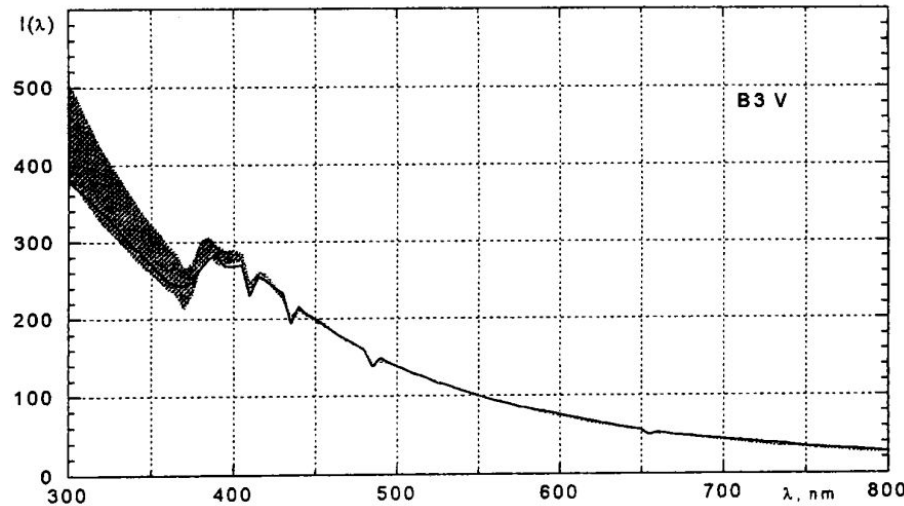


Figure: Good fit to Main Sequence stars

(Source: V. Straižys, R. Lazauskaitė and G. Valiauga, 1997)

Literature Review

2. V. Straižys, R. Lazauskaitė and G. Valiauga, 2002.

- a. Synthetically generated (metal-deficient) SED from Kurucz models - compared with that observed from real stars.
- b. Considered metal-deficient stars - BHB, F–G–K subdwarf and G–K giant types.
- c. Best coincidence found for BHB stars.
- d. Highest deviations found in UV for subdwarfs and cool metal deficient giants.
- e. T_{eff} varied by +/- 100K, $\log(g)$ and [Fe/H] varied by +/- 0.3 dex

Literature Review

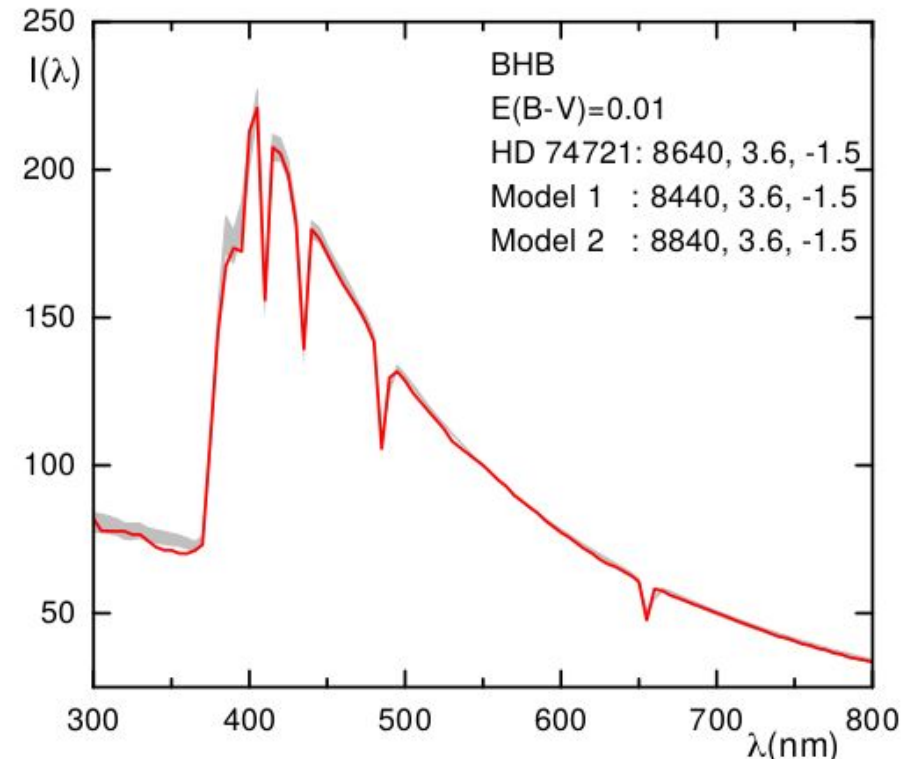


Figure: HD 74721 (BHB star) - good fit

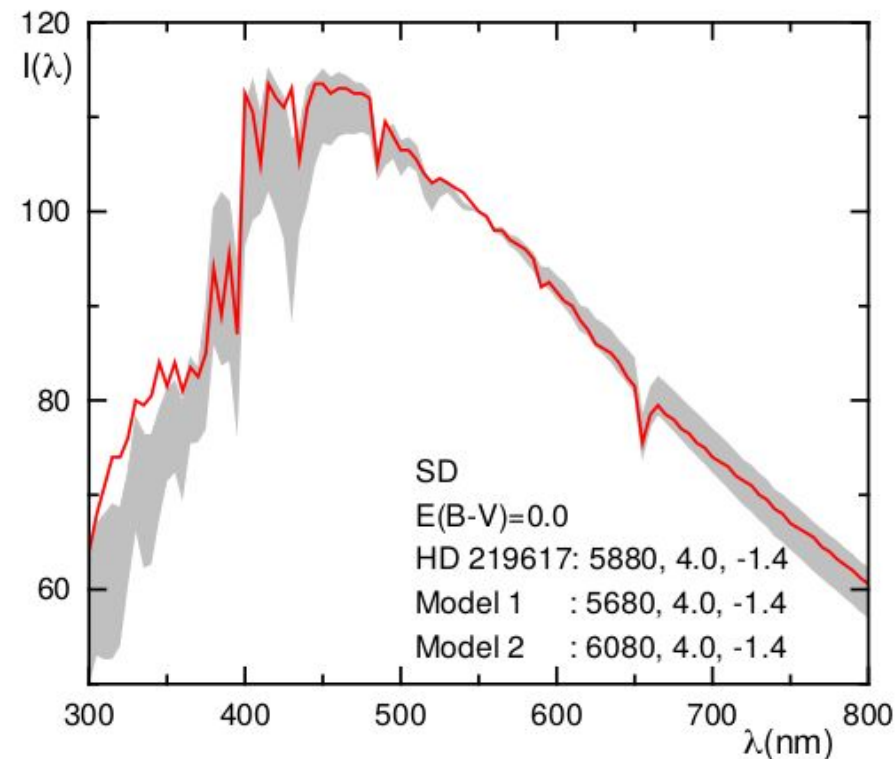


Figure: HD 219617 (subdwarf) - poor fit in UV

(Source: V. Straižys, R. Lazauskaitė and G. Valiauga, 2002)



Theory

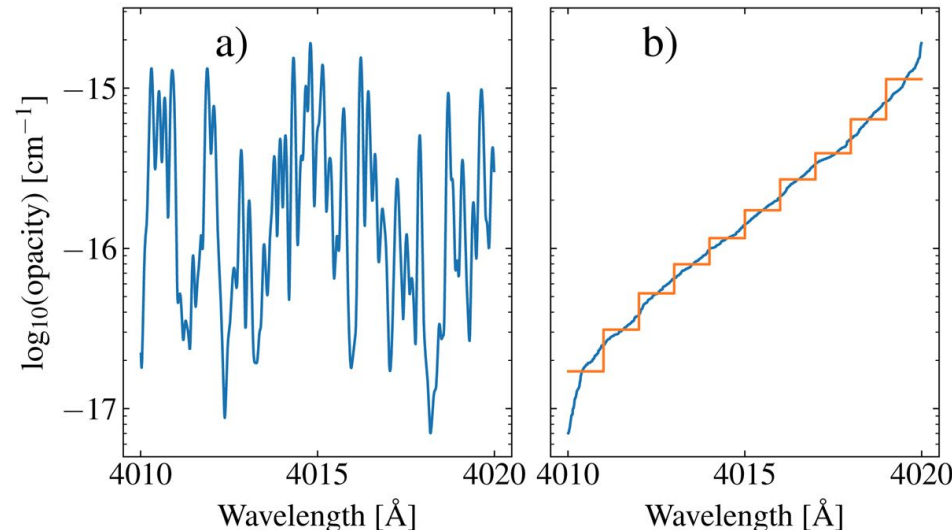
Theory

Kurucz Models Basic Assumptions:

1. Plane Parallel Approximation
$$\frac{H_{\odot}}{R_{\odot}} = \frac{kTR_{\odot}}{GM_{\odot}m_p} \approx \frac{173.2}{696340} \approx 2.5 \times 10^{-4} \ll 1$$
2. Steady State Approximation
3. Hydrostatic Equilibrium - no relative motion between layers
4. Local Thermodynamic Equilibrium - no net macroscopic energy flux within system
5. Isolated Star with core much smaller than star
6. Abundance and gravitational force constant throughout the atmosphere
7. Effects of magnetic field, stellar spots, granules, etc., are negligible

Theory

1. Convection - Mixing Length Theory - account for small-scale effects in convective motions
2. Different methods of treating opacity:
 - a. Opacity Sampling Method (ATLAS12)
 - b. Opacity Distribution Function (ATLAS9)





Data

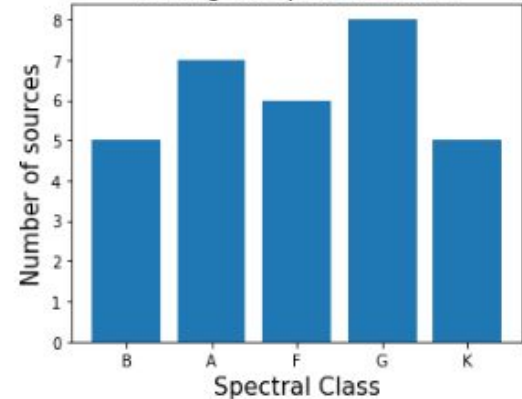
Datasets

1. STELIB:

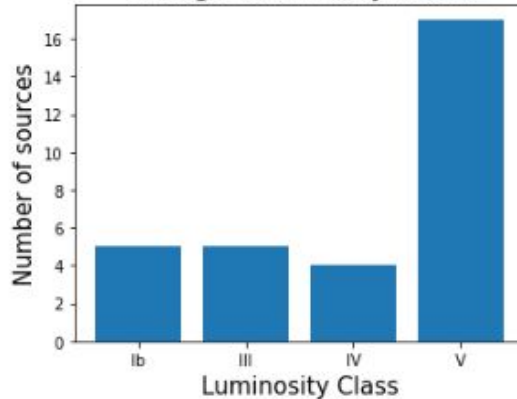
- a. 257 stellar spectra in the visible wavelength range (3200 to 9500Å)
- b. Data from 2 observatories:
 - i. 1m **Jacobus Kaptein Telescope (JKT)**, Roque de los Muchachos Observatory, Spain - Richardson-Brealey Spectrograph (600 lines/mm grating)
 - ii. 2.3m of the ANU at **Siding Spring (SSO)**, Australia - Wide Field Spectrograph



Distribution of the sources from STELIB Dataset among the spectral classes



Distribution of the sources from STELIB Dataset among the luminosity classes

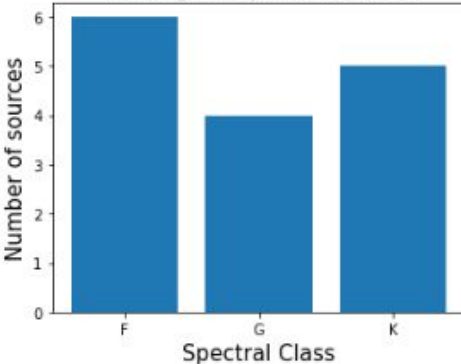


Datasets

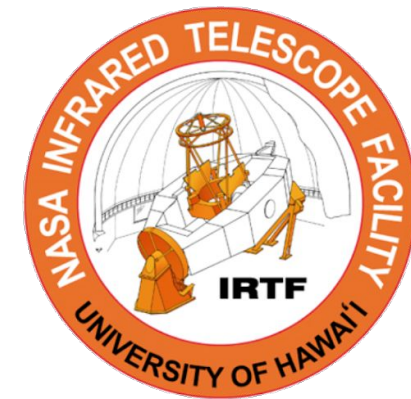
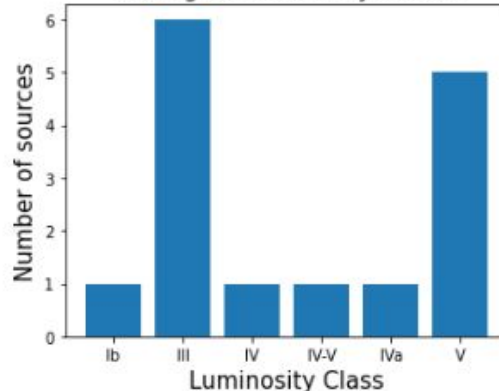
2. IRTF Spectral Library:

- a. Instrument: SpeX, medium-resolution spectrograph, at the **NASA Infrared Telescope Facility (IRTF)** on Mauna Kea.
- b. Features of the library include:
 - i. A spectral range of 0.8 to 2.5 μm (a subset from 0.8 to 5.2 μm)
 - ii. R~2000 from 0.8 to 2.5 μm and R~2500 from 2.5 to 5.2 μm
 - iii. S/N ~ 100 at $\lambda < 4 \mu\text{m}$
 - iv. Spectra shifted to zero radial velocity.

Distribution of the sources from IRTF Dataset among the spectral classes



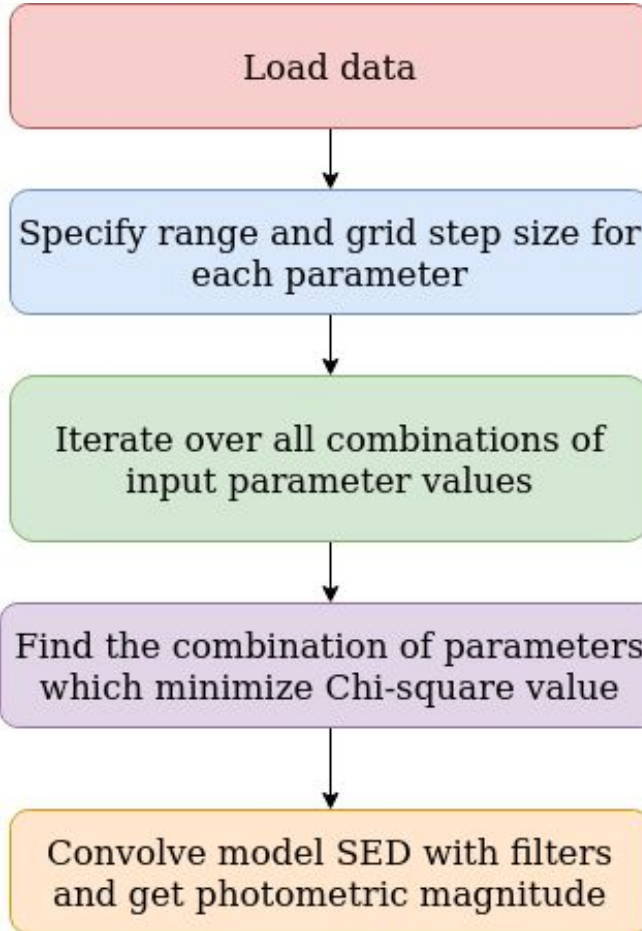
Distribution of the sources from IRTF Dataset among the luminosity classes





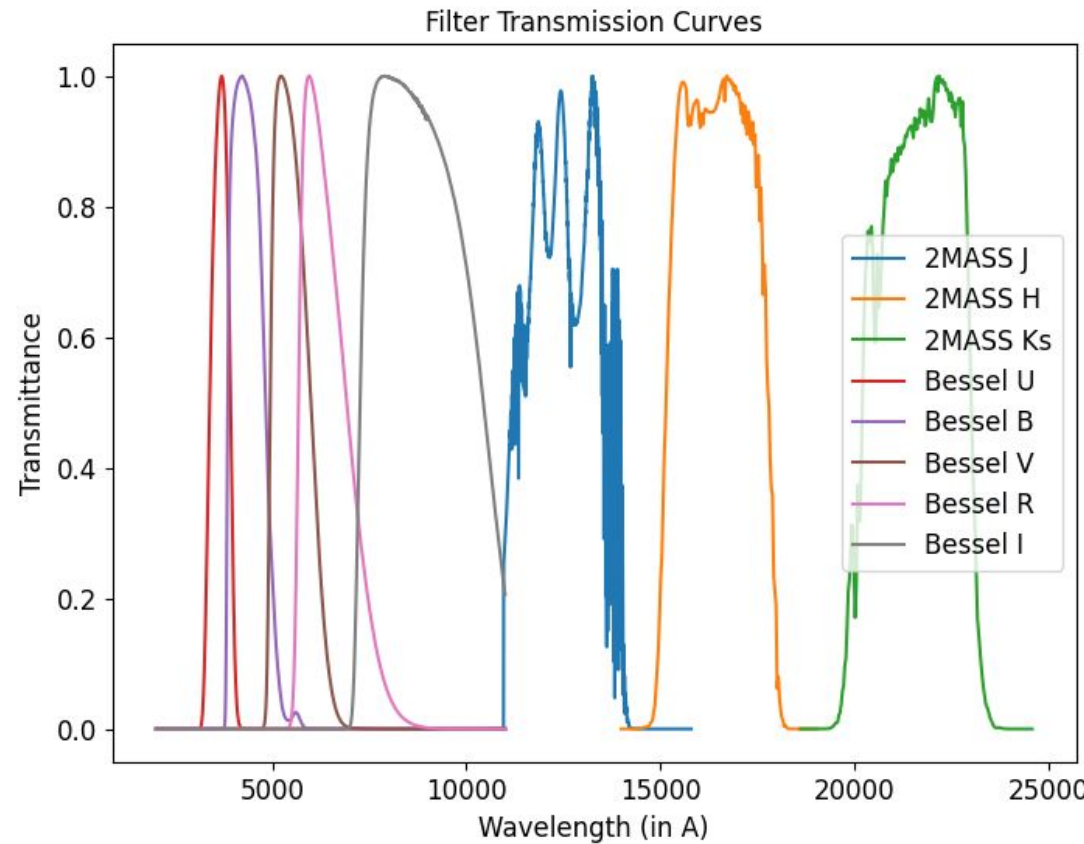
Methodology

Methodology



1. Mismatch between photometric magnitude from synthetic SED and published values - partly due to difference in filters used.
2. Grid Search - likely to miss the optimal solution due to choice of parameter range and finite grid step size.
3. Not advisable to use small grid step sizes - model inaccuracies and interpolation errors
4. Evaluation metrics:
 - a. Chi-Square value
 - b. % Residual value

Methodology



1. Model flux distribution convolved with filter transmission curves to obtain photometric magnitudes
2. $m = -2.5\log_{10}(F/F_{\text{ref}})$
3. Absolute Magnitude determined using distance estimate
4. Radius - Dilution factor and distance estimate
 - a. Distance estimate from parallax values (SIMBAD)



Implementation

Implementation



ck04models



↑ up one level

ckm05

ckm10 → ckm10

ckm15

ckm20

ckm25

ckp00

ckp02

ckp05

AA_README

catalog.fits

↑ up one level

ckm10_10000.fits
ckm10_10250.fits
ckm10_10500.fits
ckm10_10750.fits
ckm10_11000.fits
ckm10_11250.fits
ckm10_11500.fits
ckm10_11750.fits
ckm10_12000.fits

1. All data analysis performed using Python (Jupyter Notebook).
2. **PySynphot** - Python library for accessing model flux distributions
3. Models with same abundance in same directory - model spectra stored in FITS files -
 - a. designated by effective temperature
 - b. contains 12 columns - first wavelength, rest flux values at different $\log(g)$ values (0-5 in steps of 0.5) in $\text{erg/s/cm}^2/\text{A}$
4. Functions:
 - a. **Icat**: produces interpolated model flux distribution
 - b. **cat**: produces nearest model flux distribution
5. **Spectres**: Useful to obtain interpolated flux values with interpolated uncertainty values

Implementation

6. Photometric magnitudes determined using characteristics of UBVRI photometric system.
7. Mass determined using $\log(g)$ estimated - high deviation from published values.
8. Radius - fit parameter - $M_d = (R/D)^2$
9. Uncertainty in parameter estimation -
 - a. Teff, $\log(g)$ and [Fe/H] - half grid step size
 - b. Radius - max of half grid step size and uncertainty from propagation of errors from uncertainty in distance
10. Absolute Magnitude: $M = m + 5 - 5\log_{10}(d)$



Filter	λ_{eff} (\AA)	$\Delta\lambda$ (\AA)	F_λ ($\text{erg s}^{-1}\text{cm}^{-2}\text{\AA}^{-1}$)
U	3600	500	4.19×10^{-9}
B	4400	720	6.57×10^{-9}
V	5500	860	3.61×10^{-9}
R	6400	1330	2.25×10^{-9}
I	7900	1400	1.22×10^{-9}

Table A.8: UBVRI Photometric System Characteristics



Analysis

Analysis - STELIB Data

1. Observed high spread in parameter values of stars considered - justified to say that the selection effects (spectral classes) is low.
2. Mean residual value of fit in SED - 6 to 16 % (5.7 to 15.73%)
3. I band magnitude - found to highly mismatched in nearly all G and F type stars
4. Deviation from observed values of U, B, V and R magnitudes - low (relative to mismatch in I band)
5. Paschen series - well fit - observable from I band fit of B and A type stars

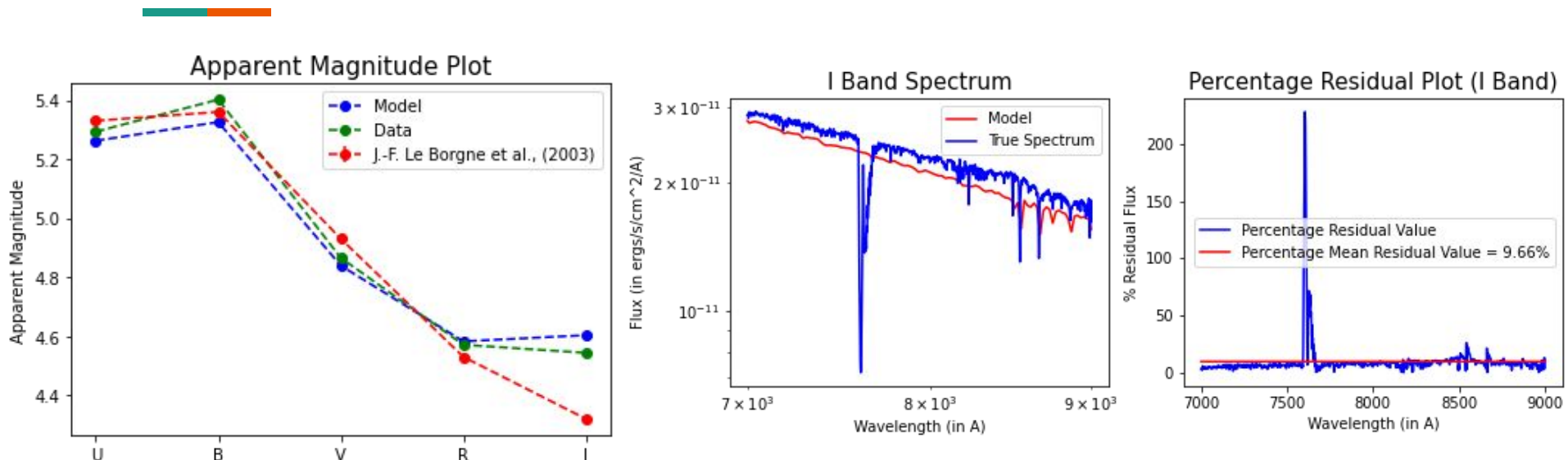
Analysis - STELIB Data

Main Sequence Stars

1. Best fit observed for F-type Main Sequence stars (~6% mean residual)
2. High deviation between model and observed SED in K-type Main Sequence Stars (~12% mean residual)
3. G-type stars - satisfactory fit (~9% mean residual)
4. Observed trend in SED of MS stars - followed by Kurucz synthetic SED - very likely to be able to fit all lines using high-resolution synthetic spectra
5. Synthetic photometry - good match in all bands - slight discrepancy in I band - possible reasons:
 - a. Model inaccuracy
 - b. Difference in filter curves

Analysis - STELIB Data

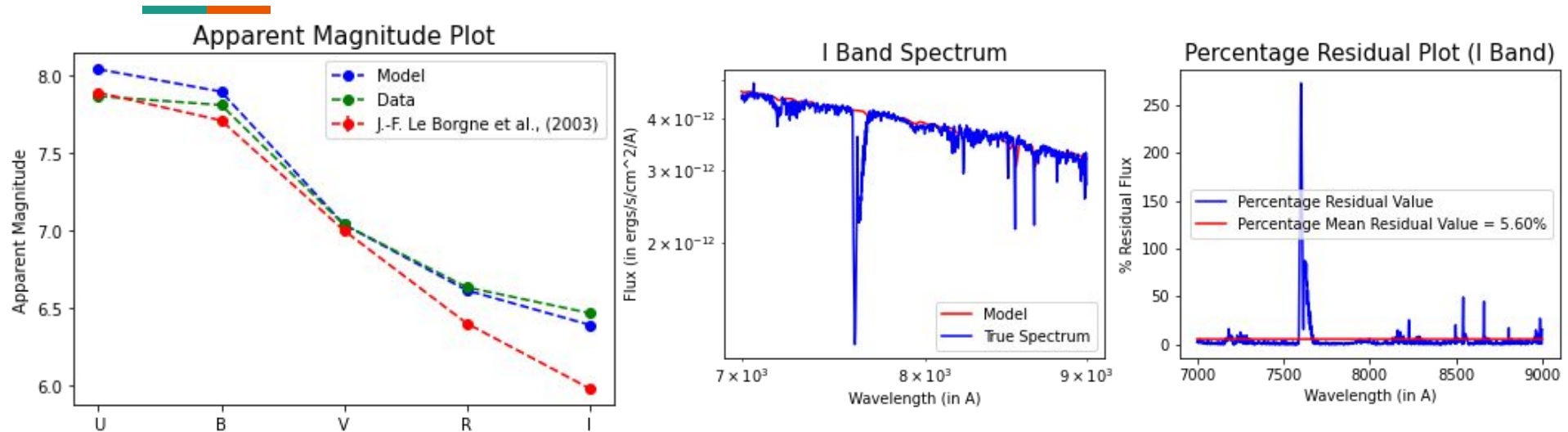
Main Sequence Stars - possible reasons for mismatch in synthetic photometry



Case - 1: HD 134083 F-type MS star - mismatch in I band photometry - model predicts lower flux than observed

Analysis - STELIB Data

Main Sequence Stars - possible reasons for mismatch in synthetic photometry

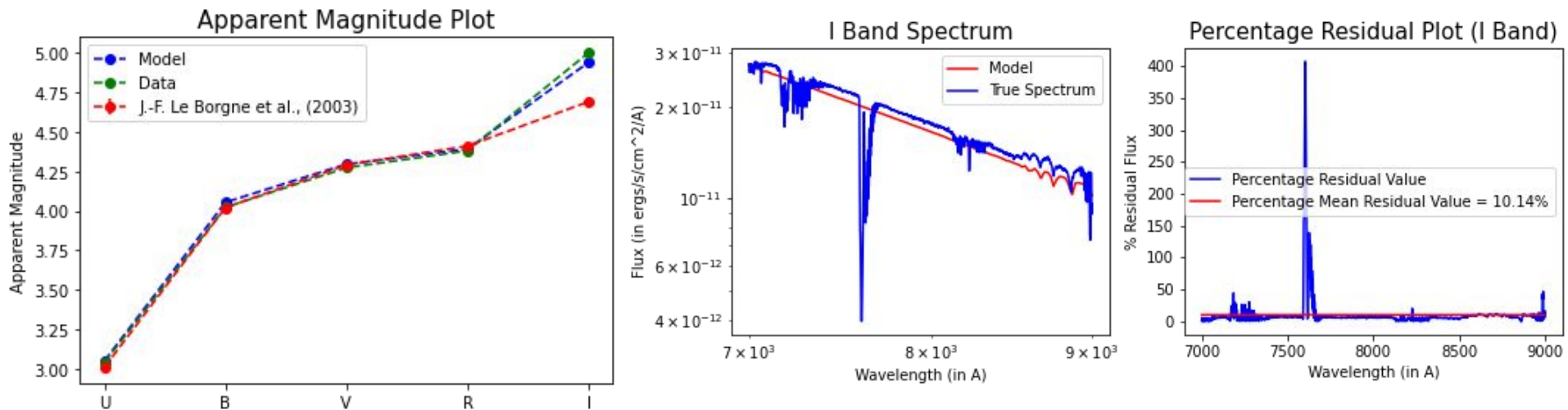


Case - 2: HD 65583 G-type MS star - mismatch in I band photometry - difference in filter transmission curves

Analysis - STELIB Data

Subgiant Stars

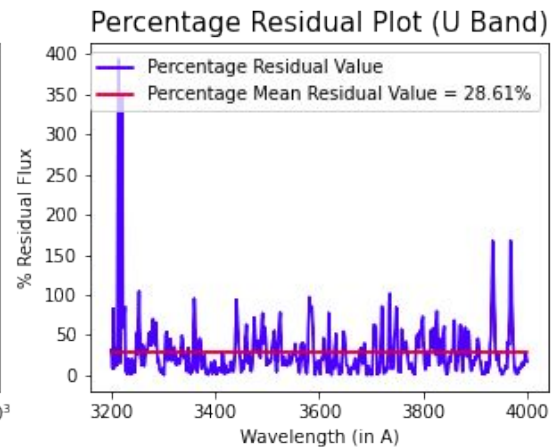
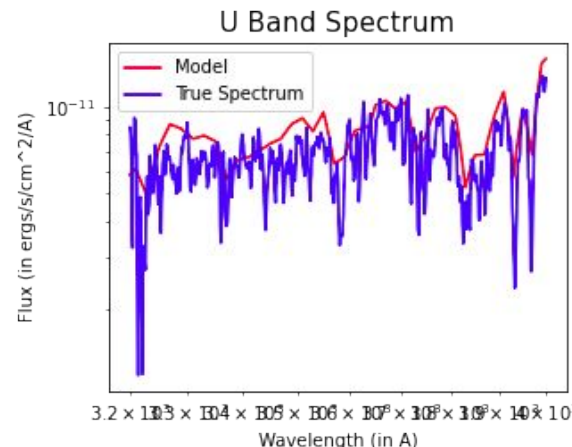
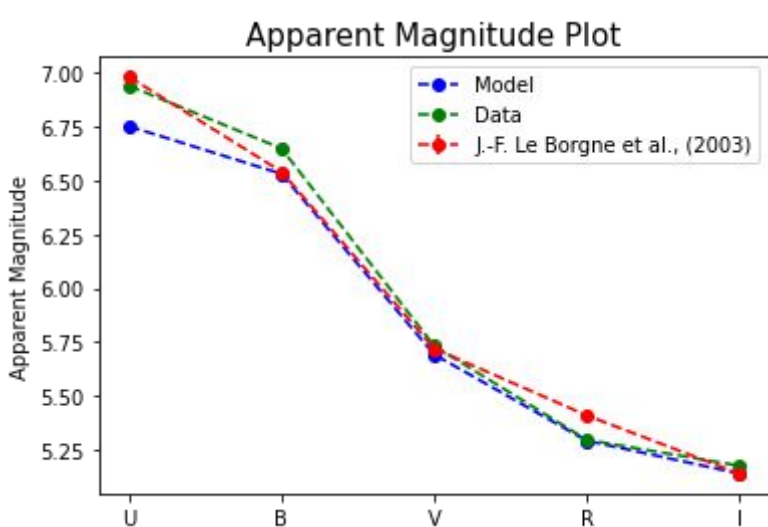
-
- 1. Good fit observed for Subgiant stars (~8-11% mean residual)
 - 2. Not sufficient number of stars in the dataset - cannot make general inferences
 - 3. Synthetic photometry - good match in all bands



HD 34816 - B0.5IV Subgiant star - filter

Analysis - STELIB Data

Subgiant Stars

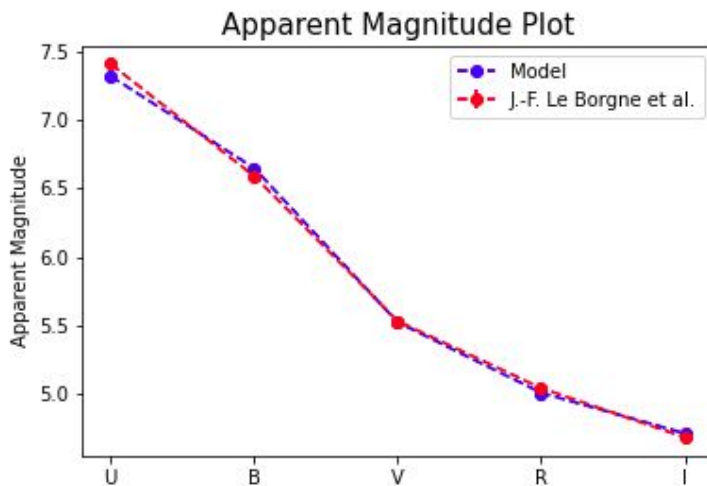


HD 67767 - G8IV Subgiant star - U Band excess flux

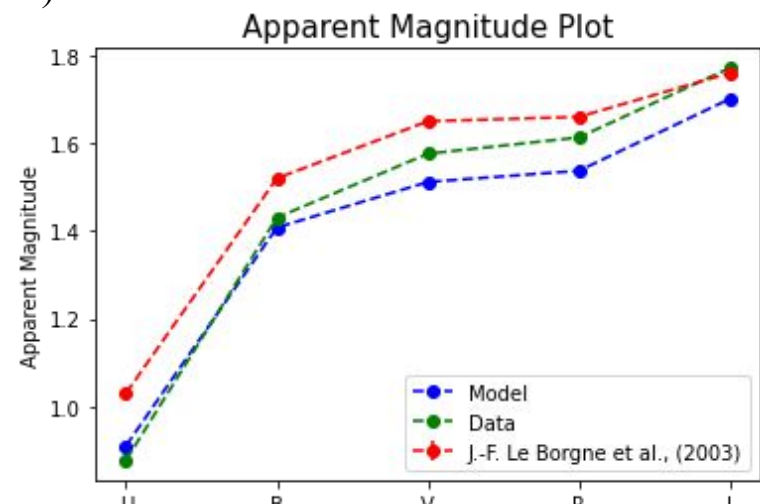
Analysis - STELIB Data

Giant Stars

-
- 1. Good fit observed for giant stars (~7-12% mean residual) - better fit in B type giants than F-K type giants
 - 2. Not sufficient number of stars in the dataset - cannot make general inferences
 - 3. Synthetic photometry - good match in all bands (+/- 0.2)



HD 100006 - K0III Giant star

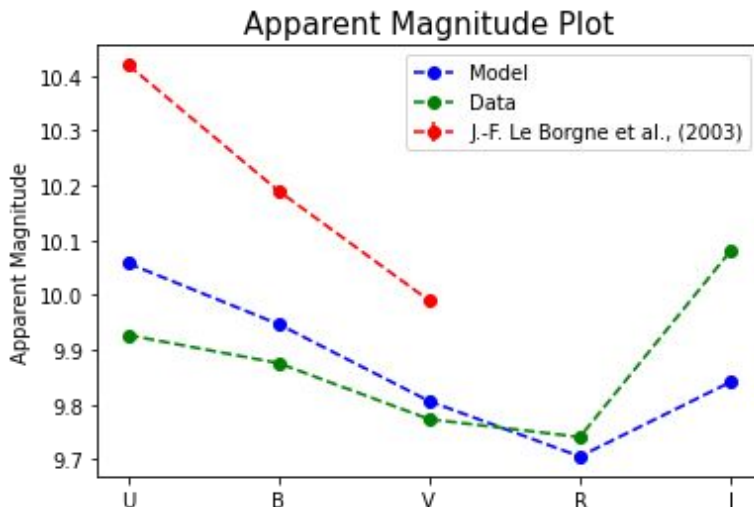


HD 35497 - B7III Giant star

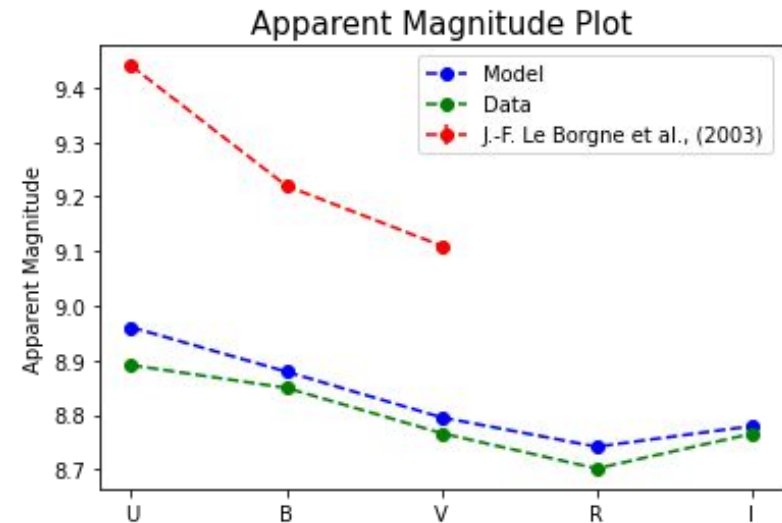
Analysis - STELIB Data

Horizontal Branch Stars

-
- 1. Good fit observed for most horizontal branch stars (~6-18% mean residual)
 - 2. Not sufficient number of stars in the dataset - to make general inferences
 - 3. Synthetic photometry - poor match to published values in all bands (deviation > 0.2)

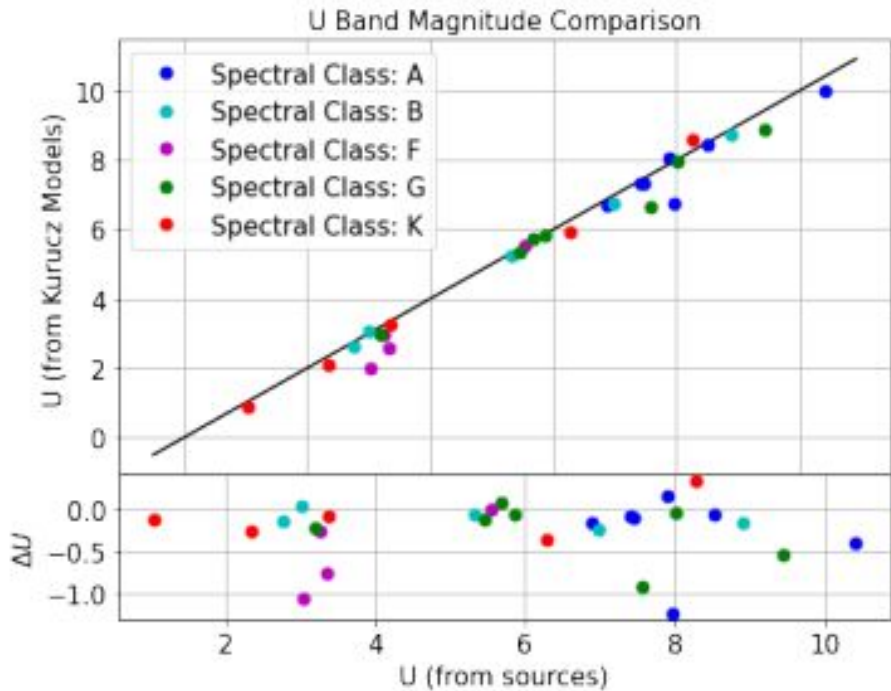


HD 2857 - A2IV HB Star

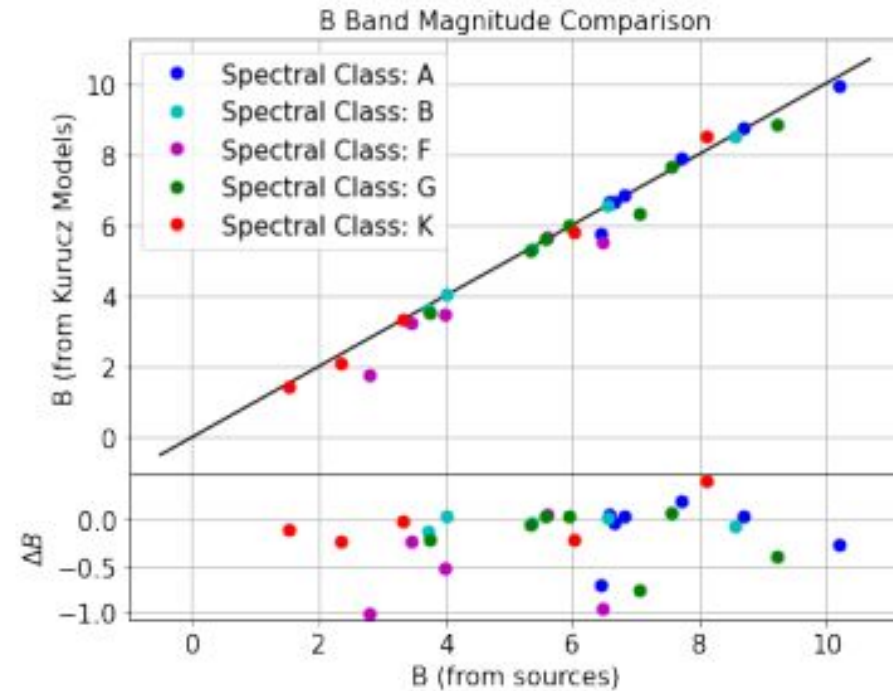


HD 60778 - A1V HB Star

Analysis - STELIB Data - Synthetic Photometry



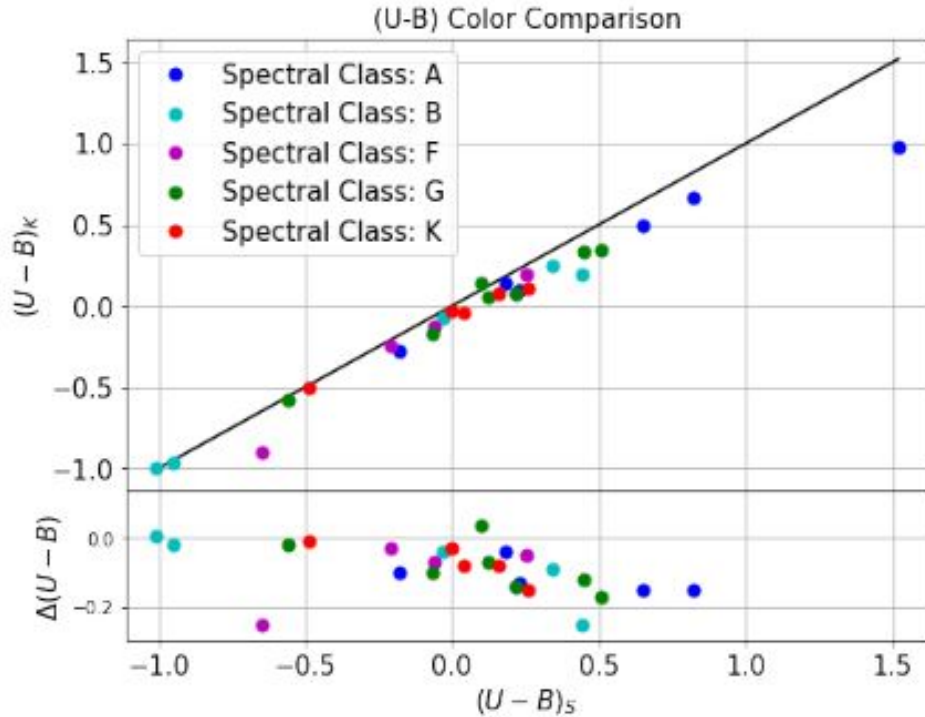
(a) U Band Magnitude Comparison



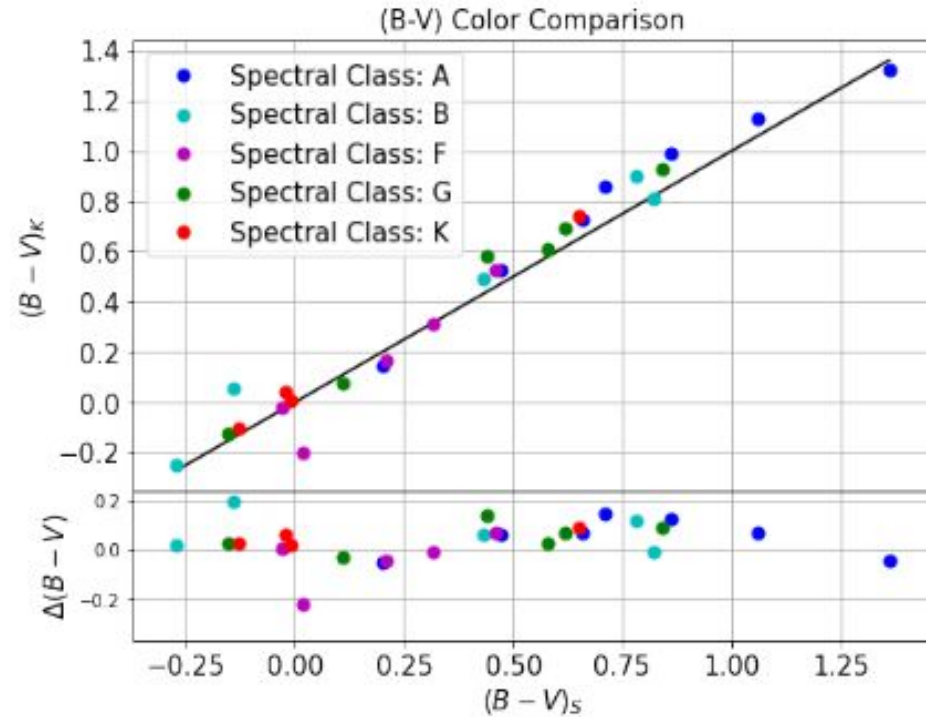
(b) B Band Magnitude Comparison

(Synthetic Photometry - good match (± 0.5) - outliers mostly due to differences in filter curves)

Analysis - STELIB Data



(a) (U-B) color comparison plot

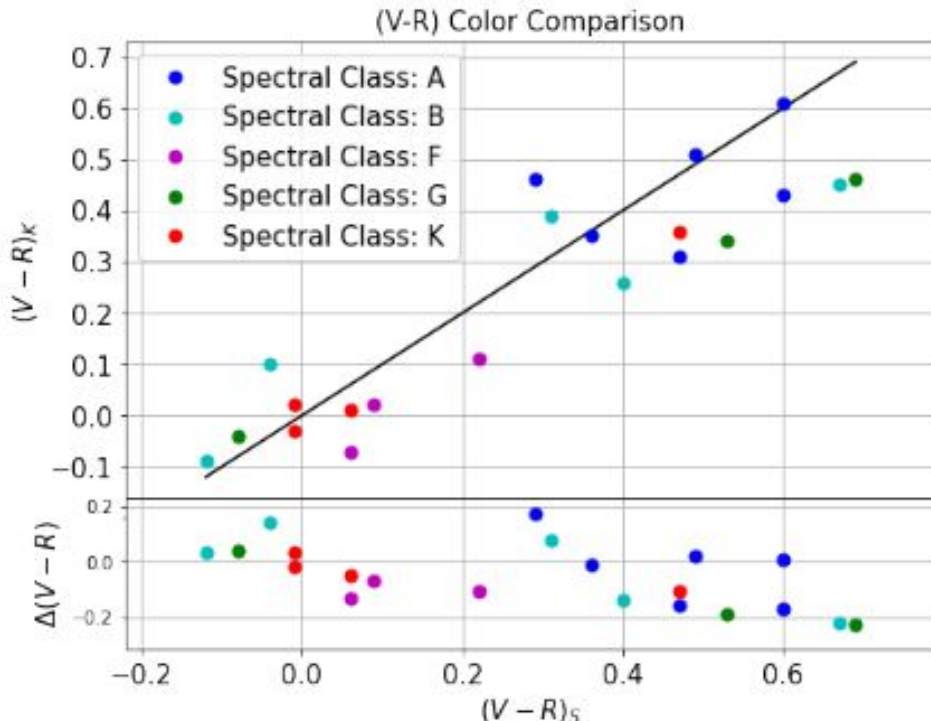


(b) (B-V) color comparison plot

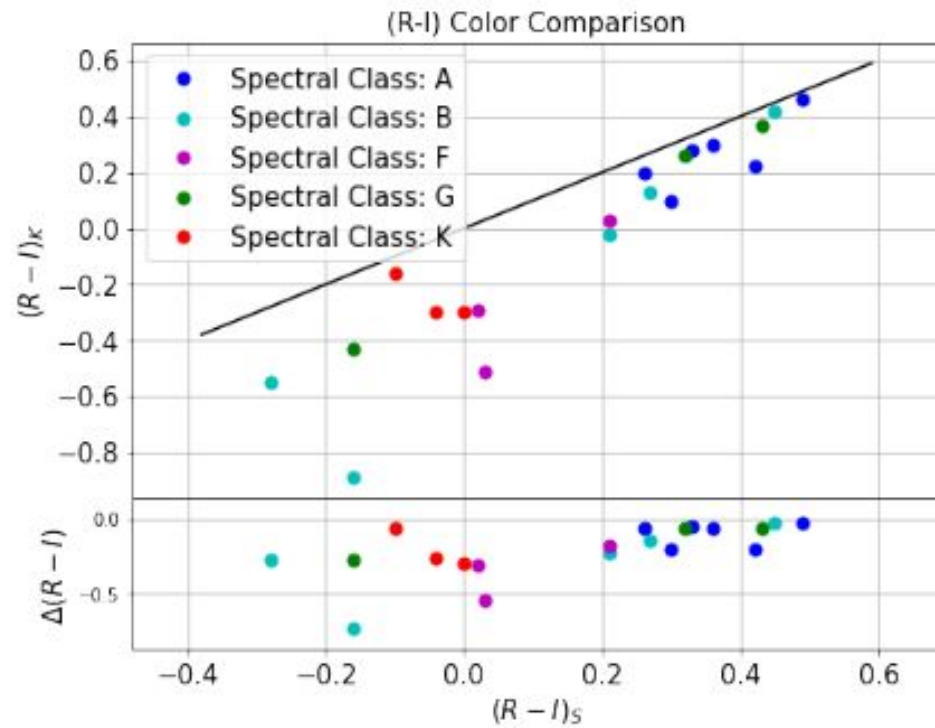
(Color-Comparison - good match (+/- 0.2))

(Inferences: for similar (but not identical) filter curves - color values match)

Analysis - STELIB Data



(c) (V-R) color comparison plot



(d) (R-I) color comparison plot

(Color-Comparison - (R-I) value underpredicted by Kurucz models)

(Inference: Near IR band color of K-type stars are underpredicted by Kurucz models)

Analysis - STELIB Data (BV only)

1. Kurucz models - fit only to
 - a. B-band spectrum
 - b. V-band spectrum
2. Observation - parameters determined from fit only to B or V bands - matches with that obtained from fit to complete spectrum
3. Deviation in fit parameters \sim grid step size
4. Spread in synthetic photometric magnitudes - similar to that obtained from overall fit

Analysis - STELIB Data (BV only)

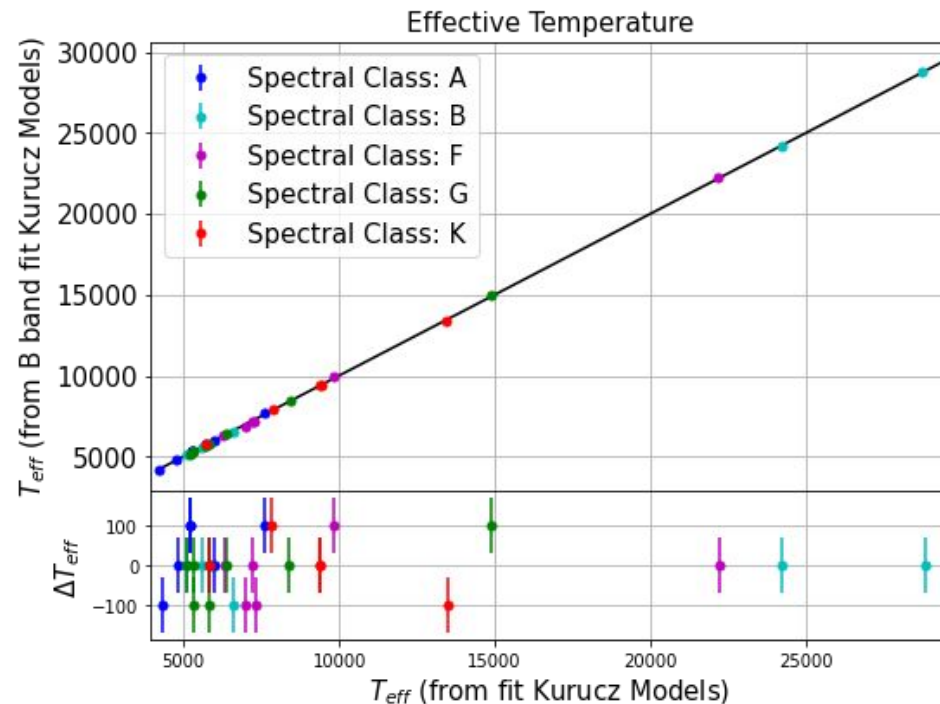


Figure: Comparison of effective temperature determined from B band fit with overall fit

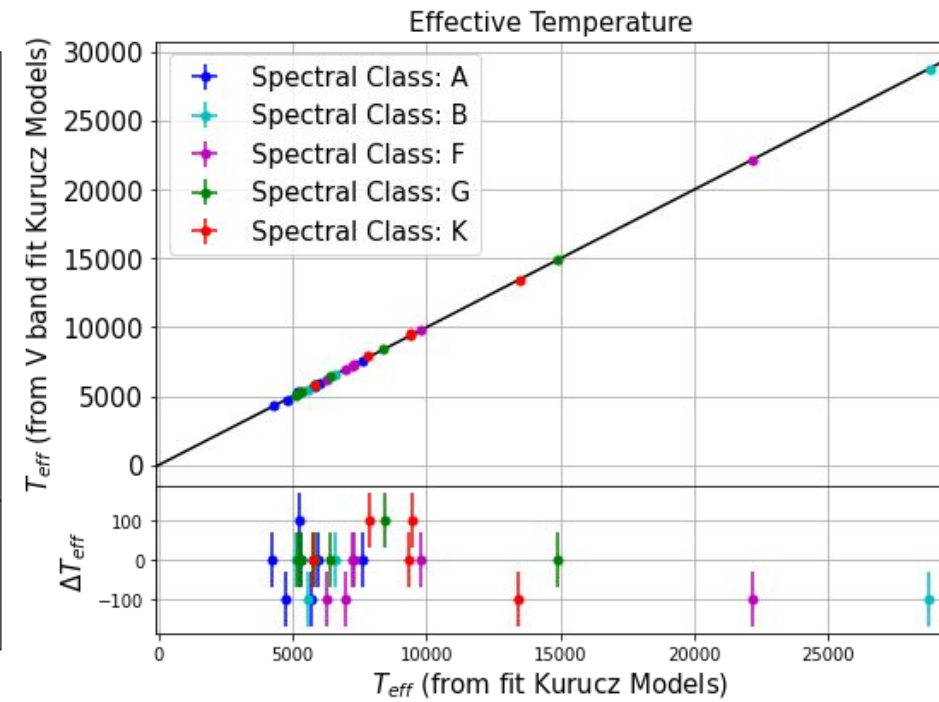


Figure: Comparison of effective temperature determined from V band fit with overall fit

Match between parameters from B/V band fit to overall fit

Analysis - STELIB Data (BV only)

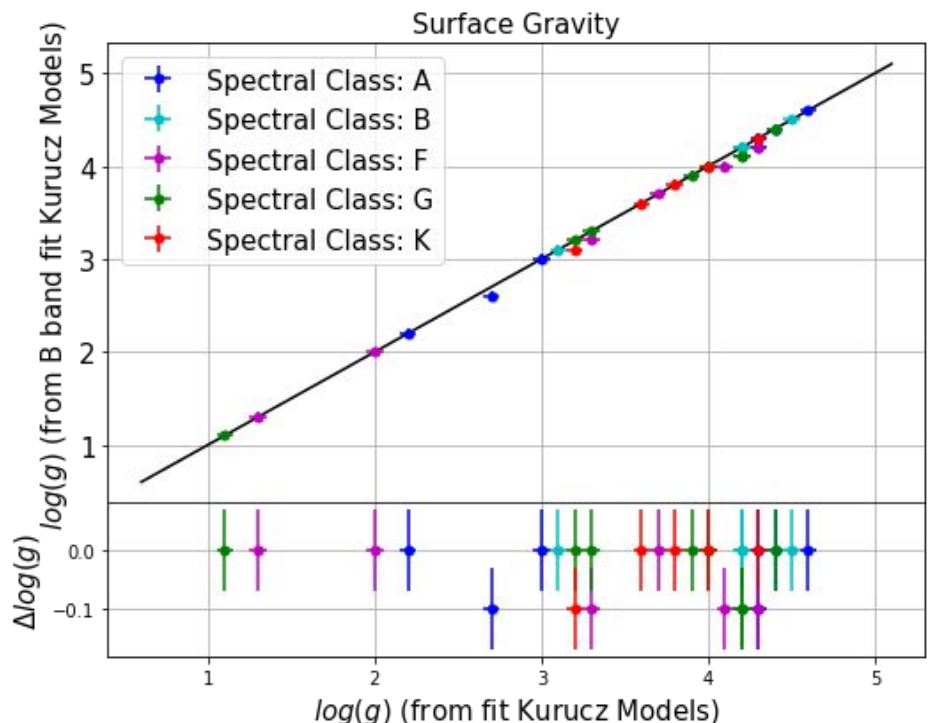


Figure: Comparison of surface gravity determined from B band fit with overall fit

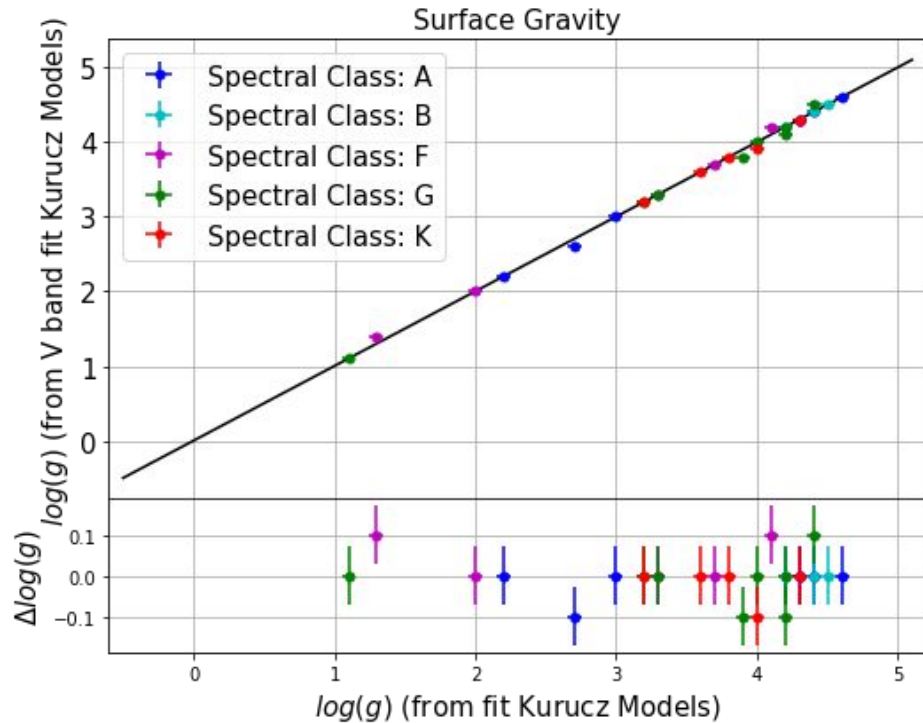


Figure: Comparison of surface gravity determined from V band fit with overall fit

Match between parameters from B/V band fit to overall fit

Analysis - STELIB Data (BV only)

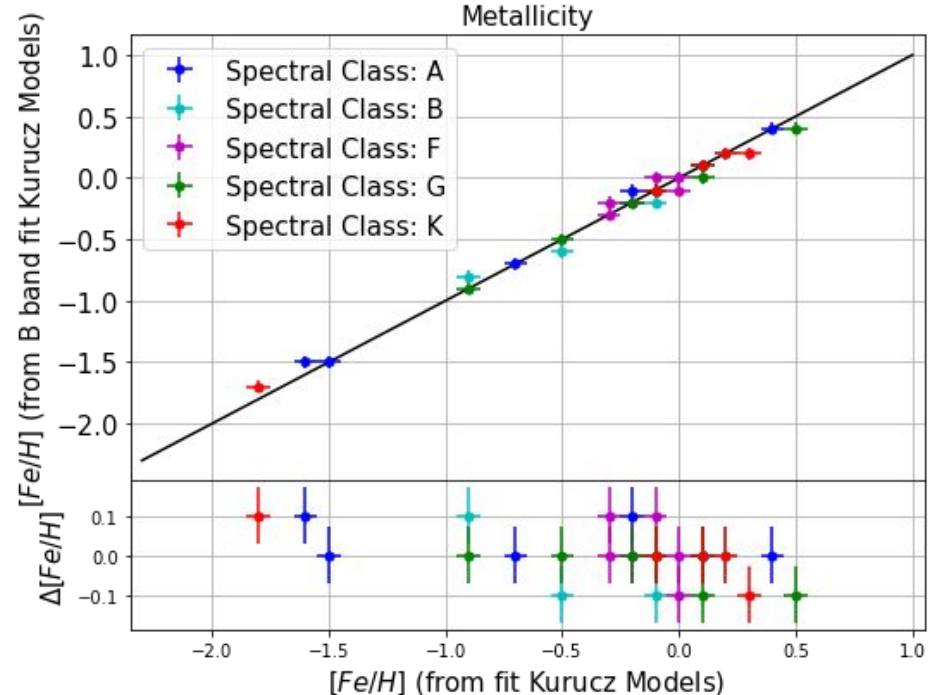


Figure: Comparison of metallicity determined from B band fit with overall fit

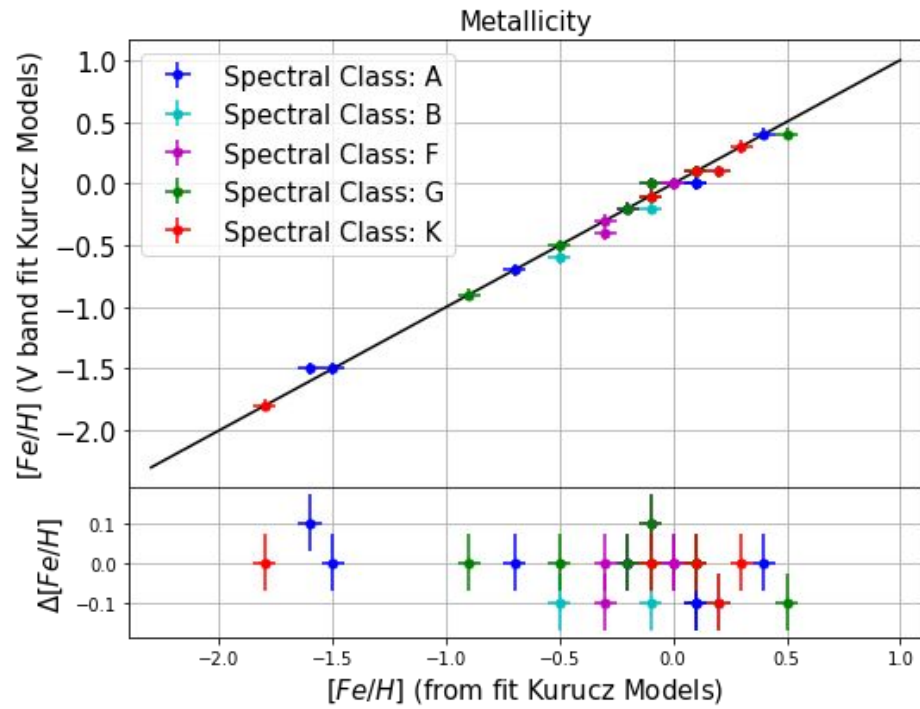
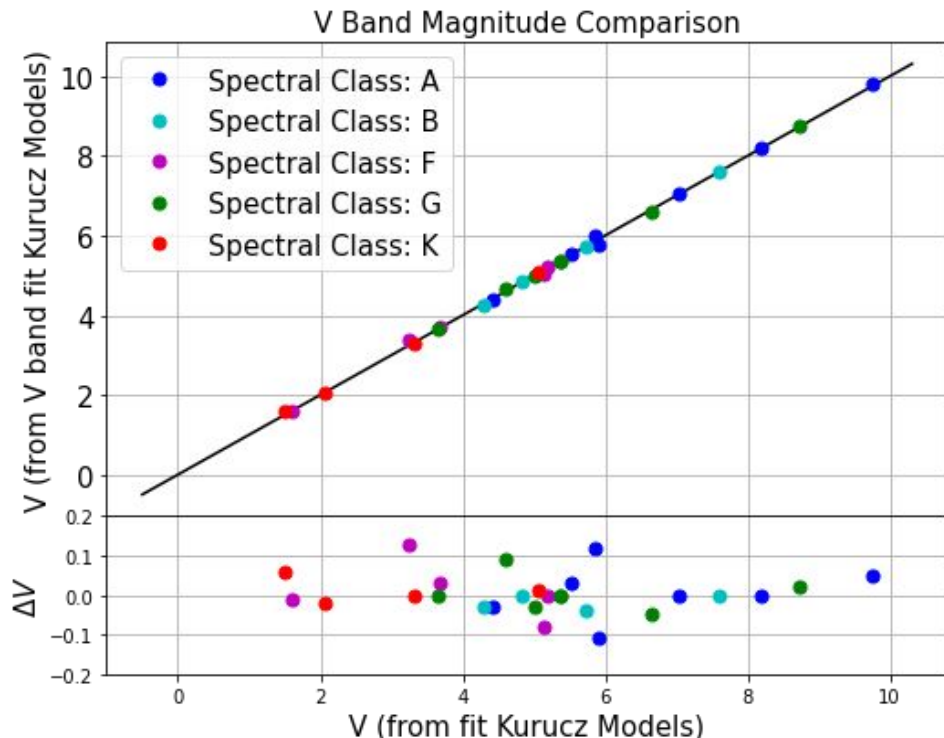
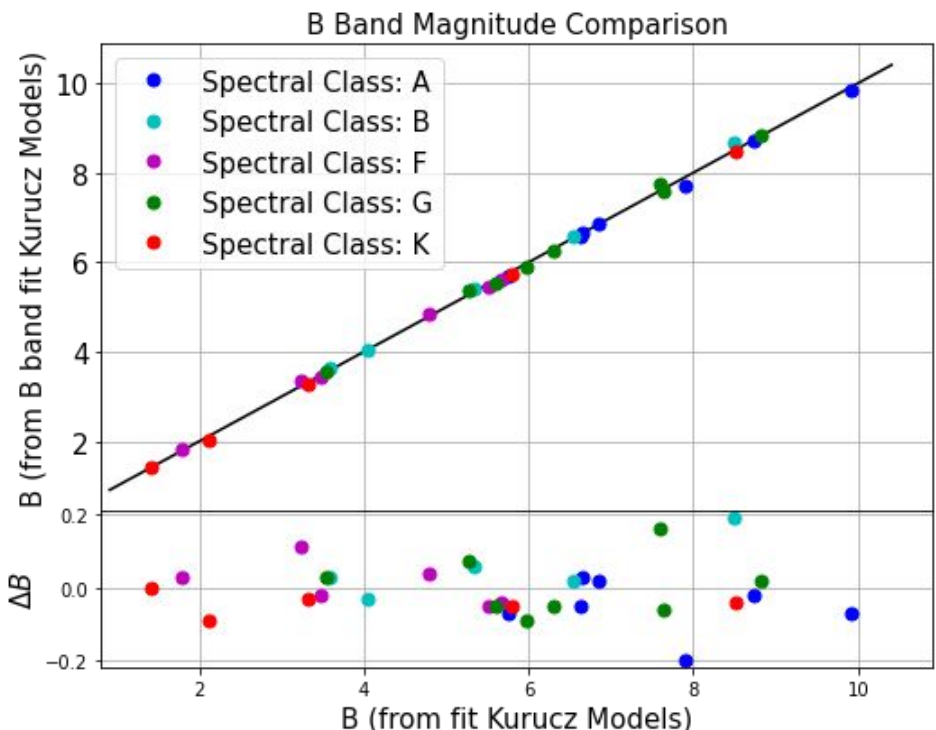


Figure: Comparison of metallicity determined from V band fit with overall fit

Match between parameters from B/V band fit to overall fit

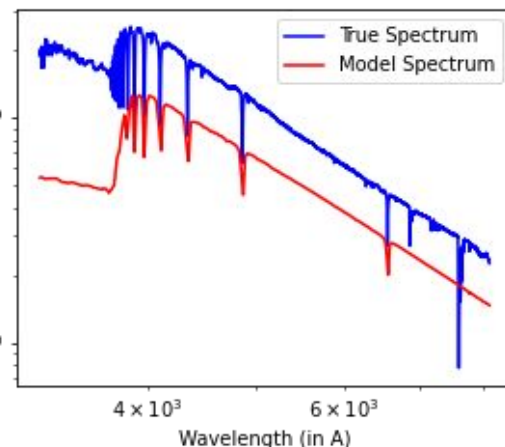
Analysis - STELIB Data (BV only)



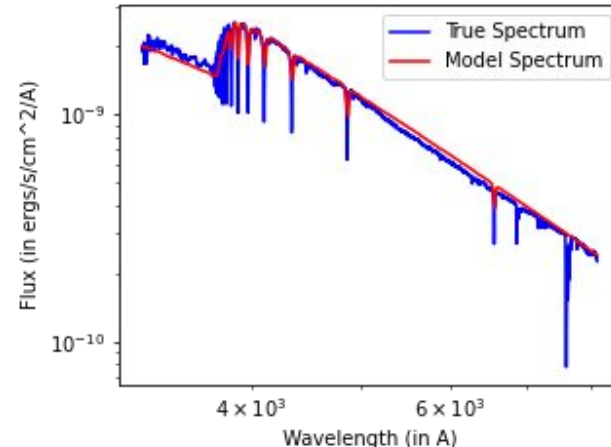
Good match in synthetic photometry from B/V band fit compared to overall fit

Effect of each parameter

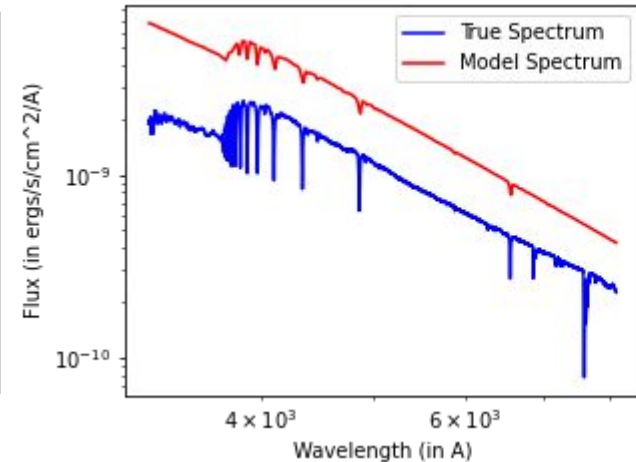
1. Effective temperature - Overall increase in flux with increase in effective temperature



Teff = 10000 K



Teff = 13500 K

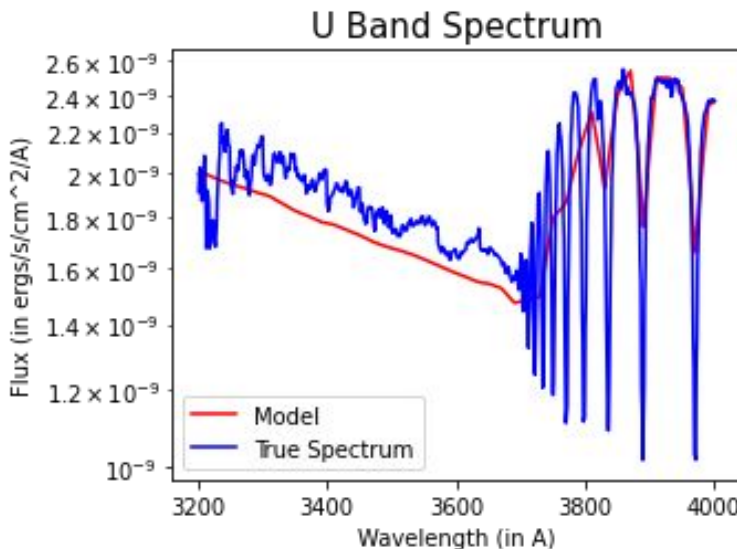


Teff = 20000 K

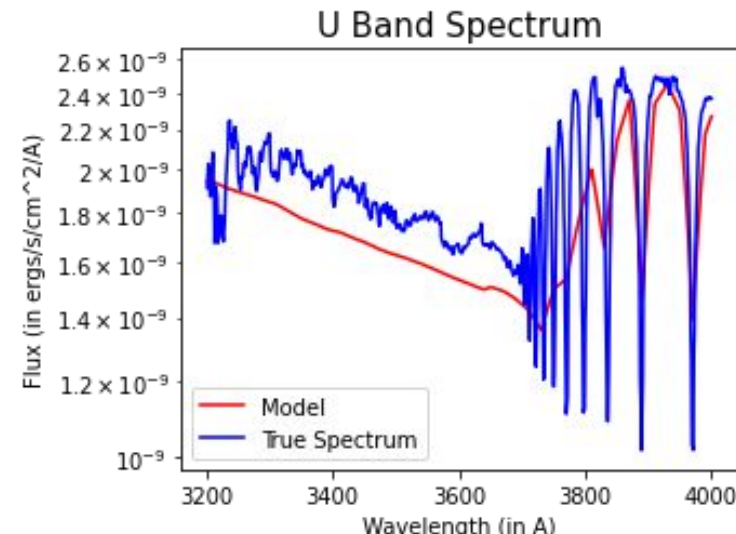
HD 35497 - B7III star

Effect of each parameter

2. Surface gravity -
 - a. No visible variation in R and I band flux
 - b. Pressure broadening - visible in prominent lines



$$\log(g) = 3.8 \text{ dex}$$



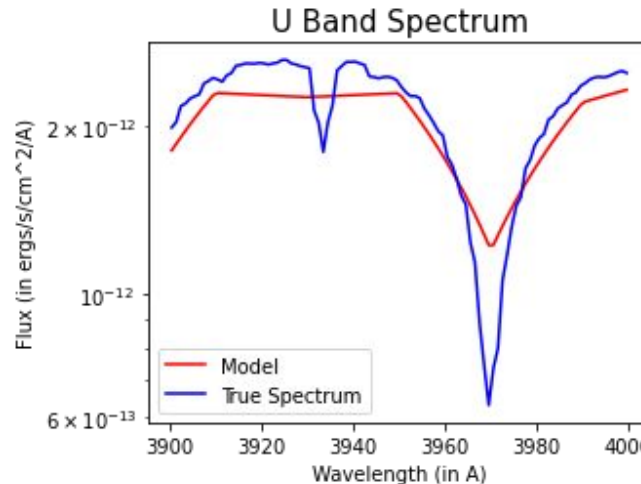
$$\log(g) = 4.8 \text{ dex}$$

HD 35497 - B7III star

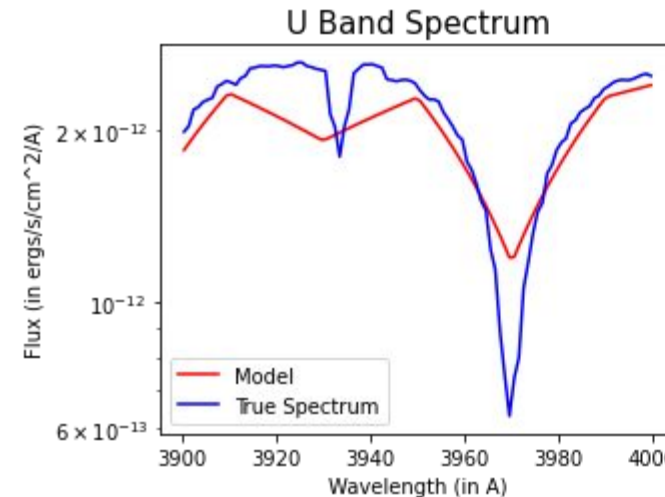
Effect of each parameter

3. Metallicity -

- a. With increase in metallicity - model SED tries to fit the Calcium K line ($\approx 3968\text{\AA}$), in the U band.
- b. Also observe an overall increase in the flux in longer wavelength range (R and I bands).



$$[\text{Fe}/\text{H}] = -0.5 \text{ dex}$$



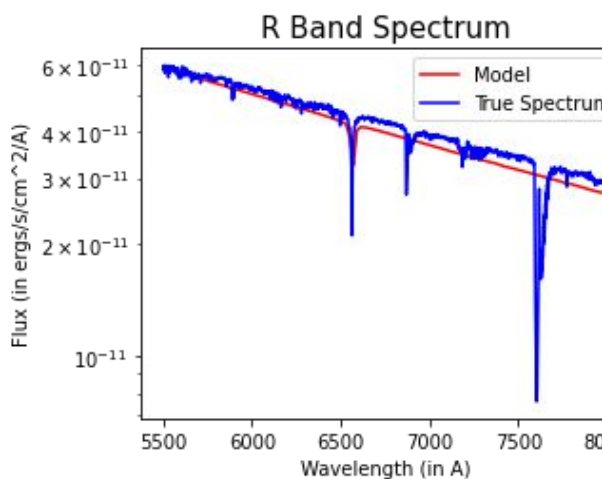
$$[\text{Fe}/\text{H}] = +0.5 \text{ dex}$$

HD 60778 - A1V star

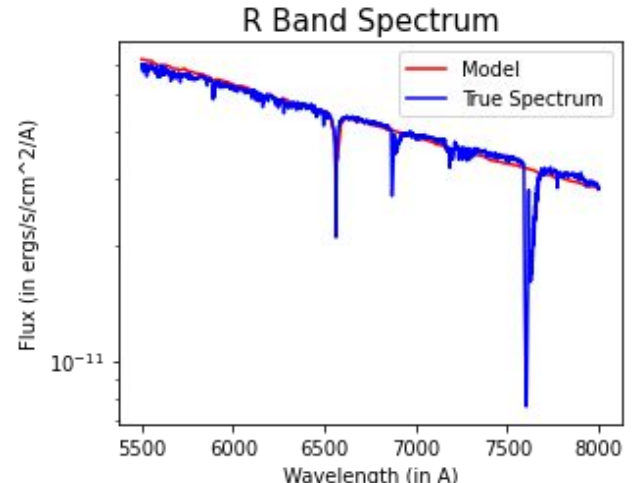
Effect of each parameter

3. Metallicity -

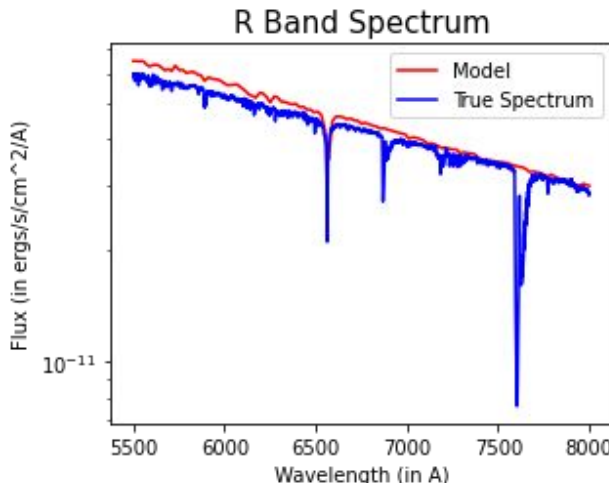
- With increase in metallicity - model SED tries to fit the Calcium K line ($\approx 3968\text{\AA}$), in the U band.
- Also observe an overall increase in the flux in longer wavelength range (R and I bands).



$[\text{Fe}/\text{H}] = -1.0 \text{ dex}$



$[\text{Fe}/\text{H}] = -0.3 \text{ dex}$



$[\text{Fe}/\text{H}] = +0.3 \text{ dex}$

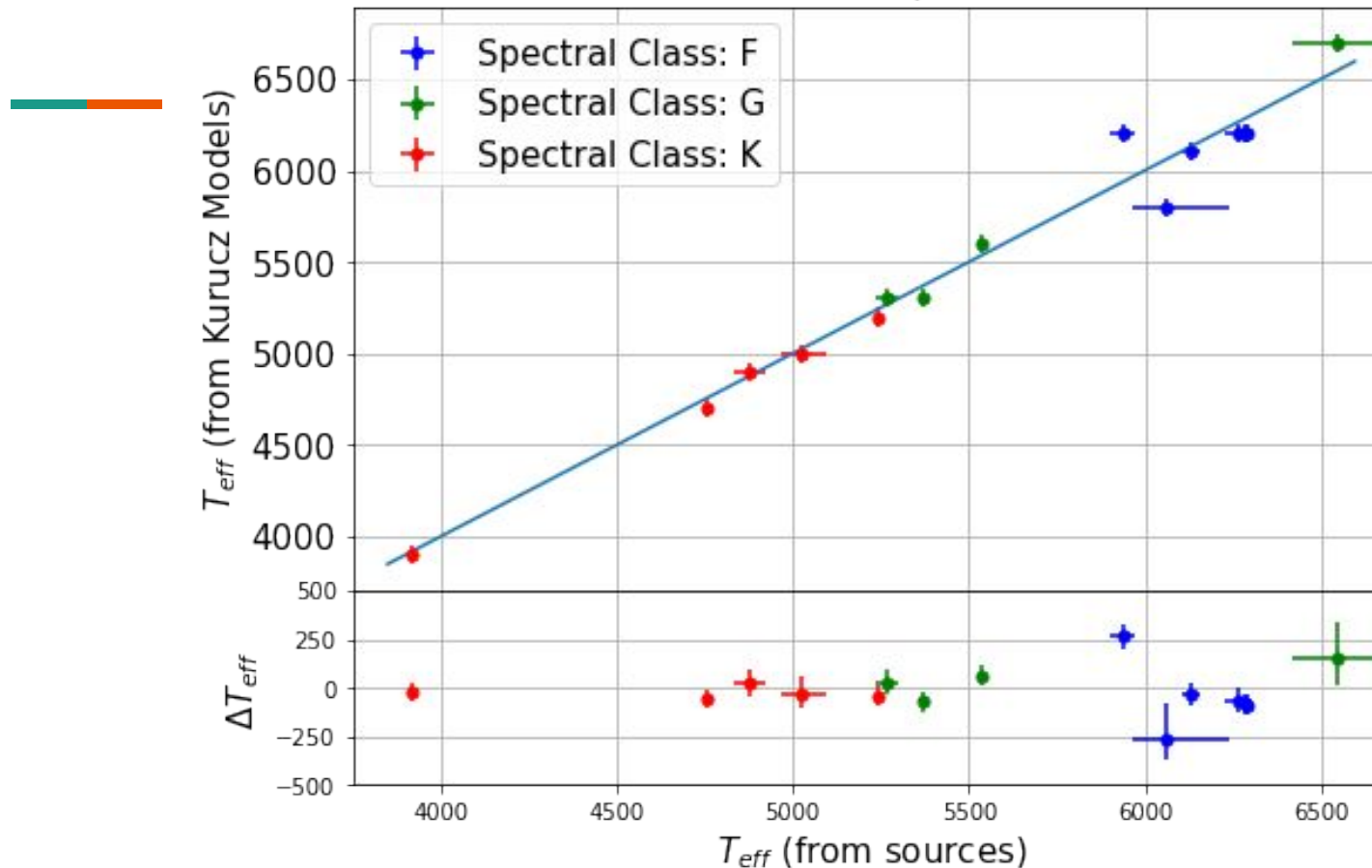
HD 32537 - F0V star

Analysis - IRTF Data

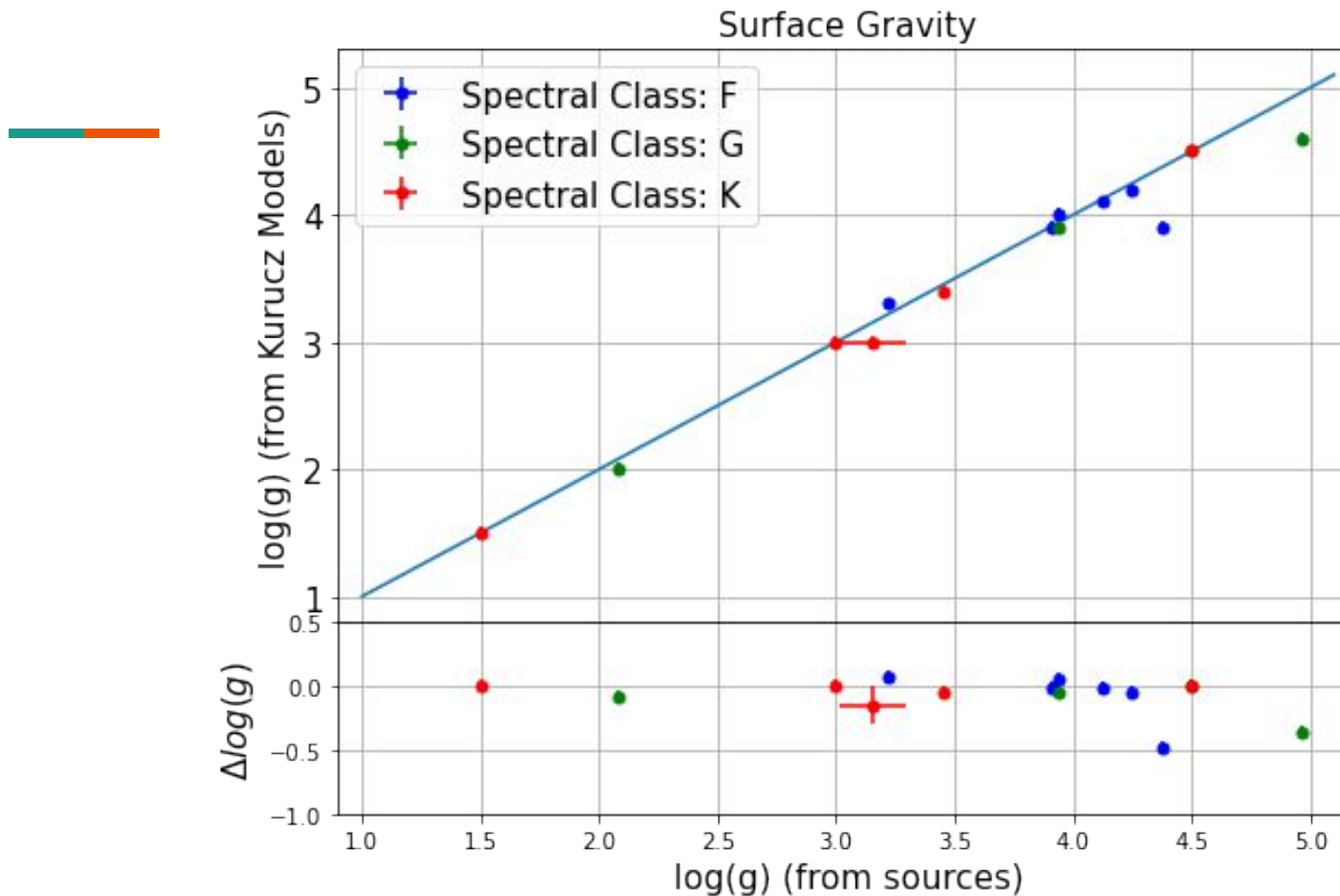
1. Good fit by Kurucz synthetic SED to observed SED in near IR bands (J, H, Ks) - mean deviation (residual) $\sim 2\text{-}6\%$ (some outliers)
2. Match between parameters:
 - a. Effective temperature - $+\text{-} 300\text{ K}$ (mostly $+\text{-} 100\text{ K}$, with outliers)
 - b. Surface gravity - $+\text{-} 0.5\text{ dex}$ (mostly under-predicted - $+\text{-} 0.2\text{ dex}$, with outliers)
 - c. Metallicity - $+\text{-} 0.1\text{ dex}$
3. Stars with near solar metallicity ($<0.05\text{ dex}$) - not all fit by model with $[\text{Fe}/\text{H}] = 0$
4. Metallicity as a free parameter - leads to un-physically values (offset from independently determined value by about 0.3 dex).

Analysis - IRTF Data

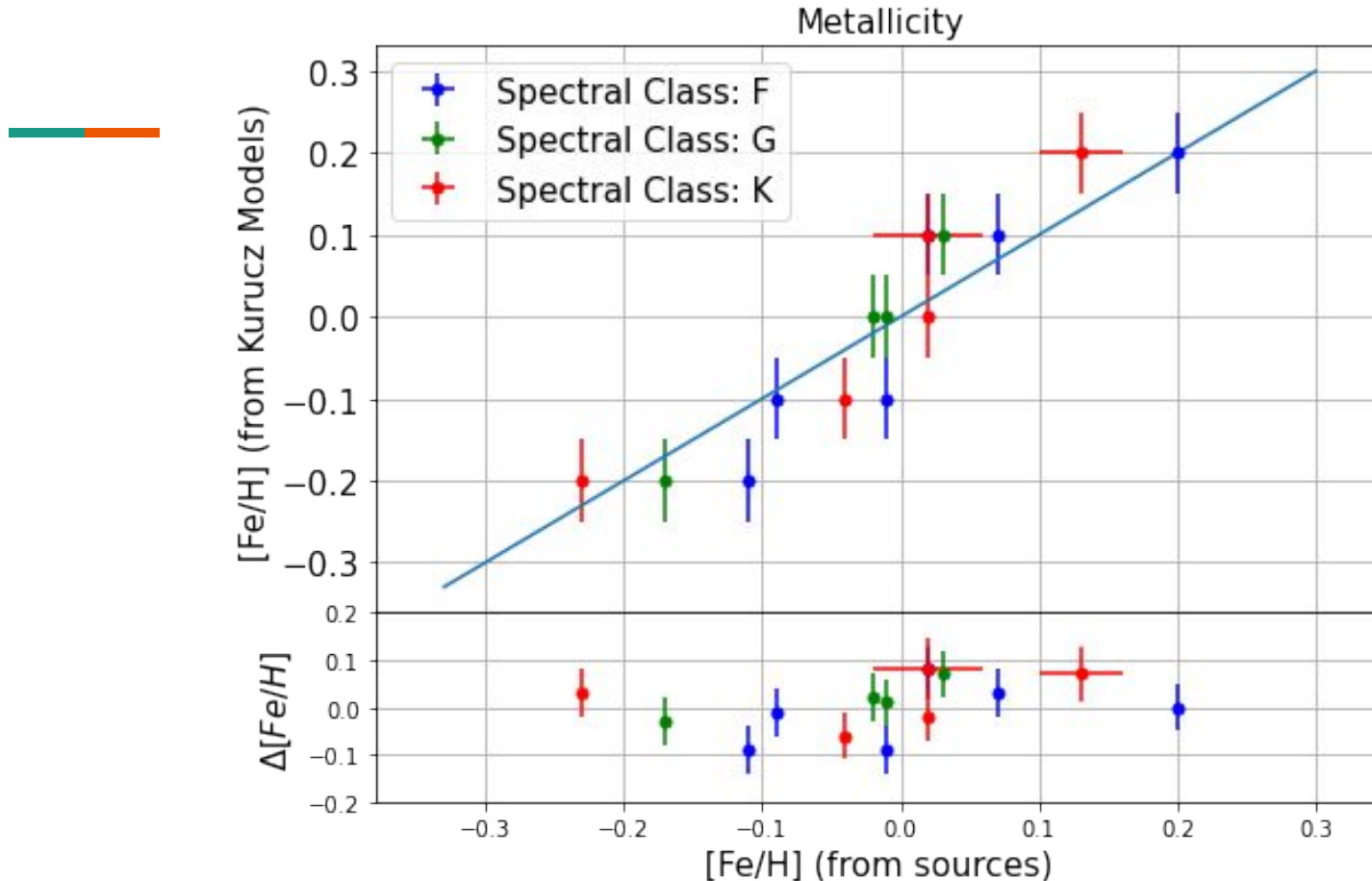
Effective Temperature



Analysis - IRTF Data



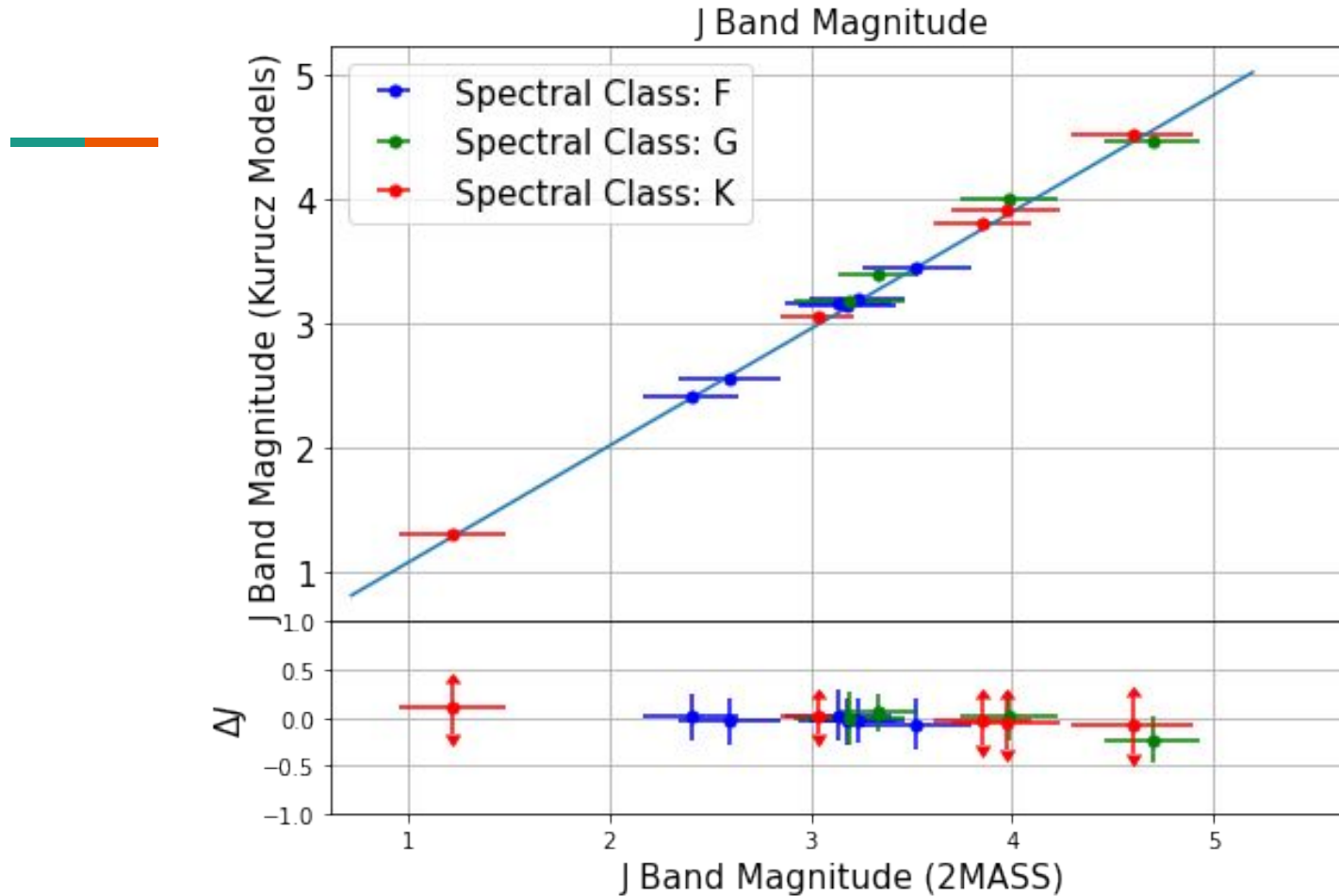
Analysis - IRTF Data



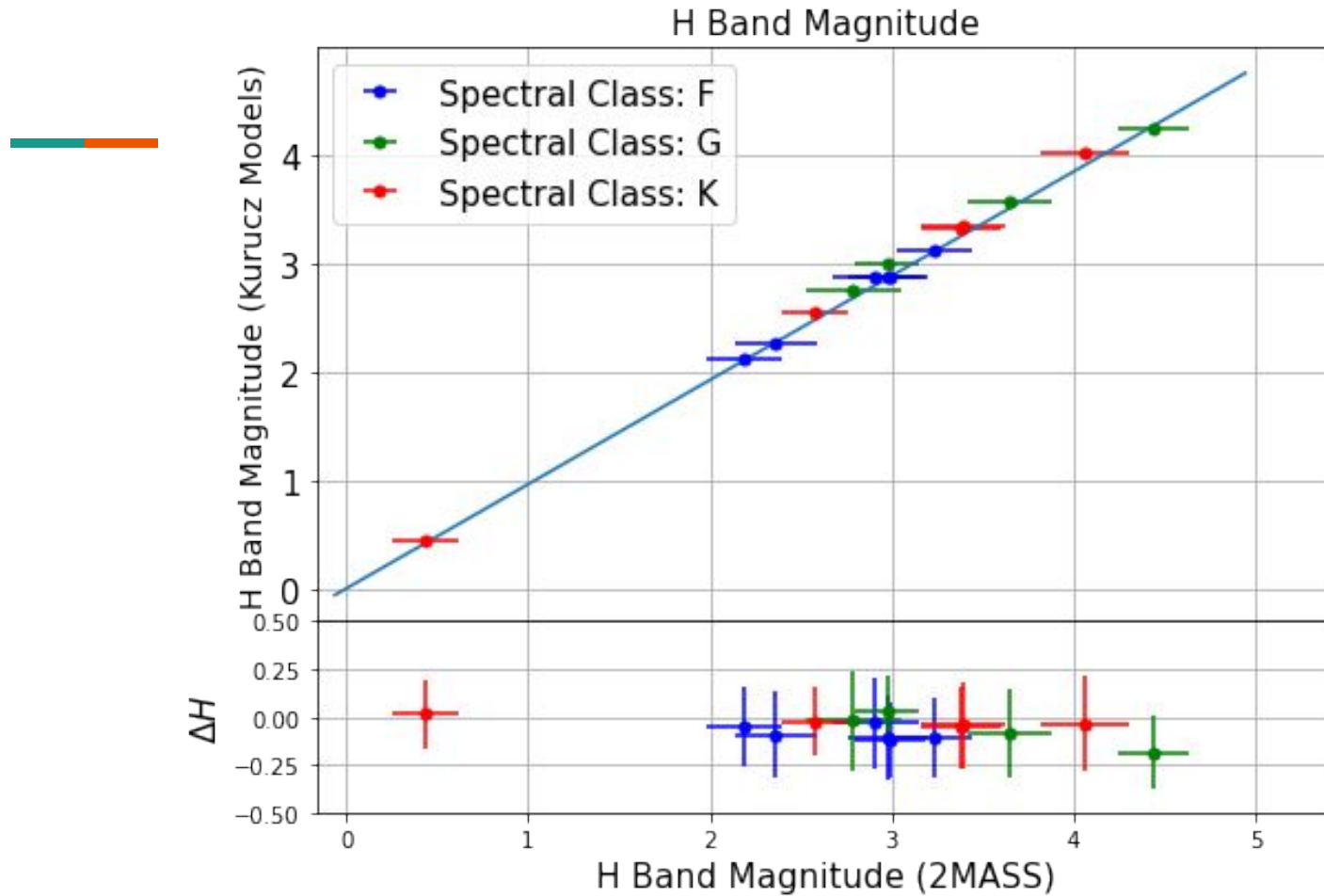
Analysis - J, H, Ks Band Synthetic Photometry

1. Synthetic photometric magnitude - well within observational error bars
2. Published photometric magnitude values - from 2MASS database
3. First order deviation in synthetic photometric magnitudes from observed values
4. Contributors to good match in photometry, partly due to:
 - a. Identicalness of the filter curves used for synthetic photometry and observational photometry
 - b. Good fit by Kurucz synthetic SED to observational SEDs in near IR bands (J, H, Ks) - mean deviation (residual) $\sim 2\text{-}3\%$ (with some outliers)

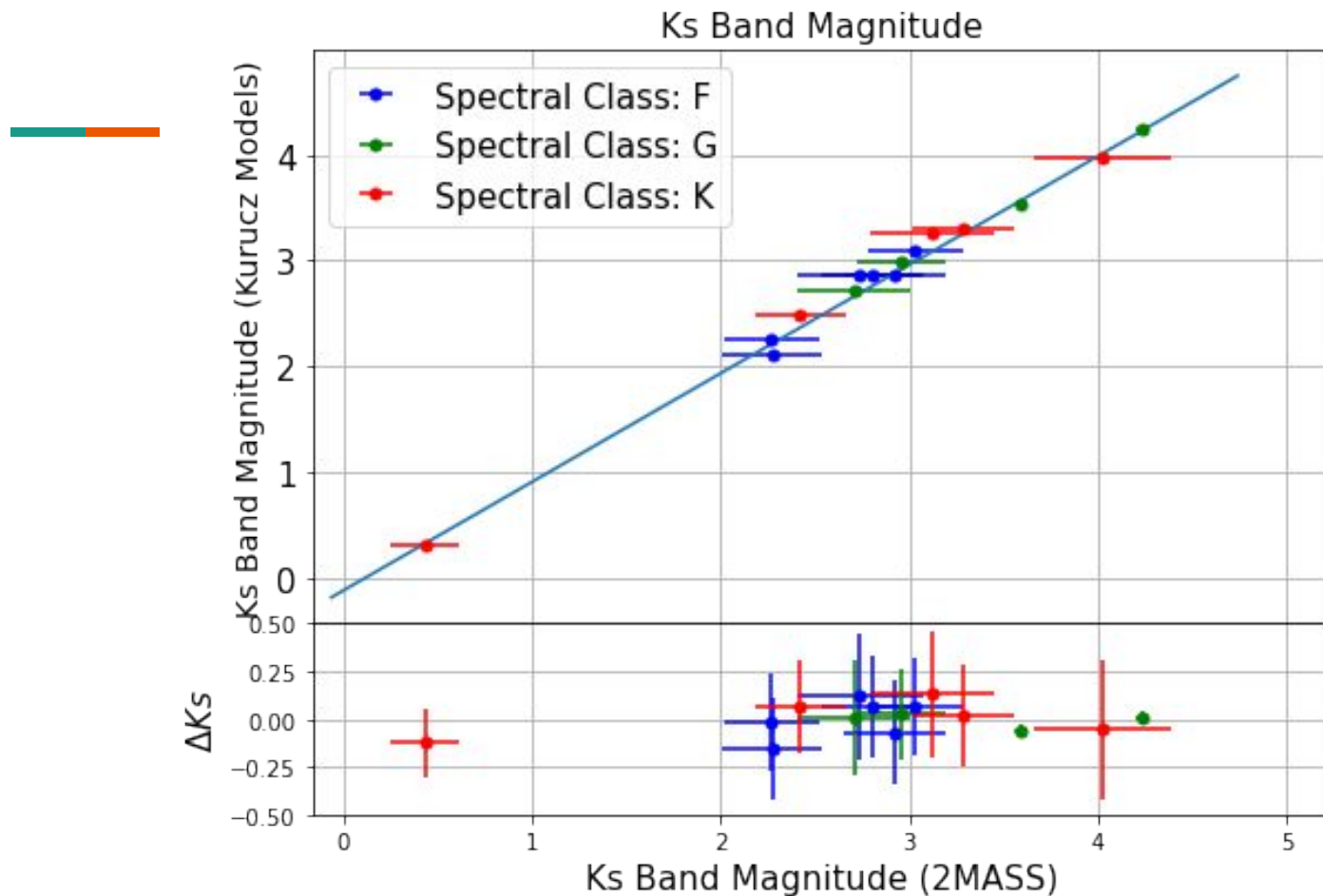
Analysis - J Band Magnitude Comparison



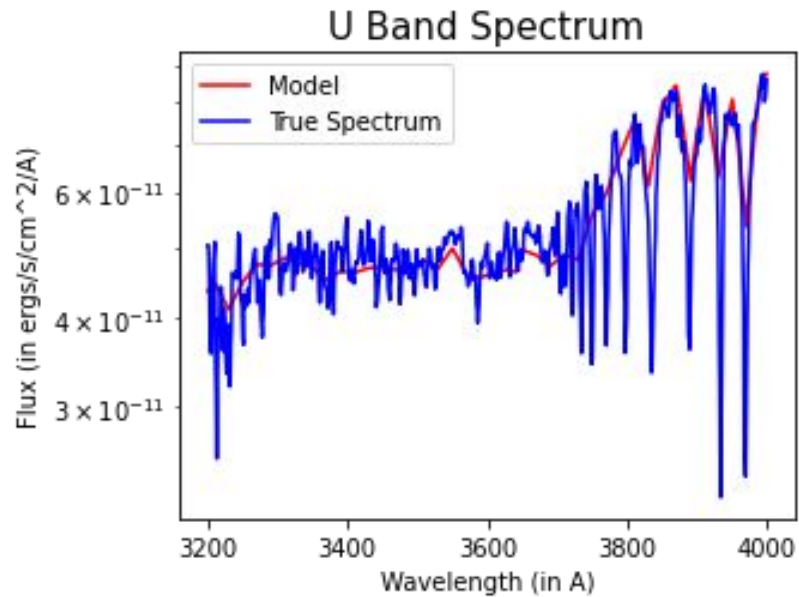
Analysis - H Band Magnitude Comparison



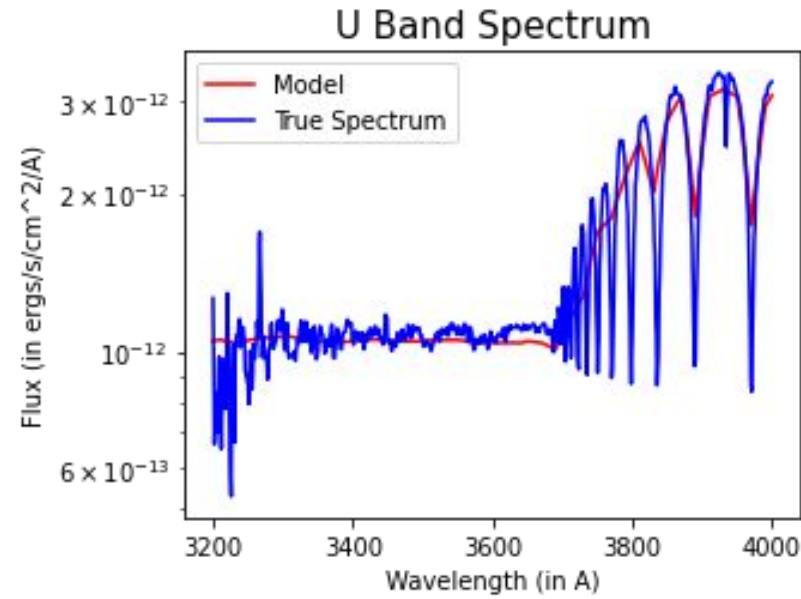
Analysis - Ks Band Magnitude Comparison



Analysis - Hydrogen spectral series



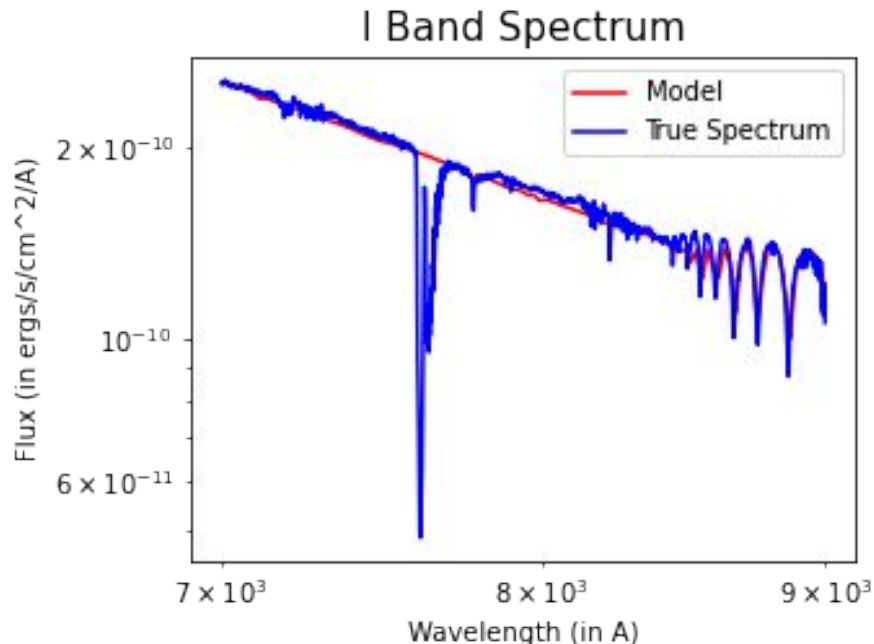
(HD 32537: F0V Star)



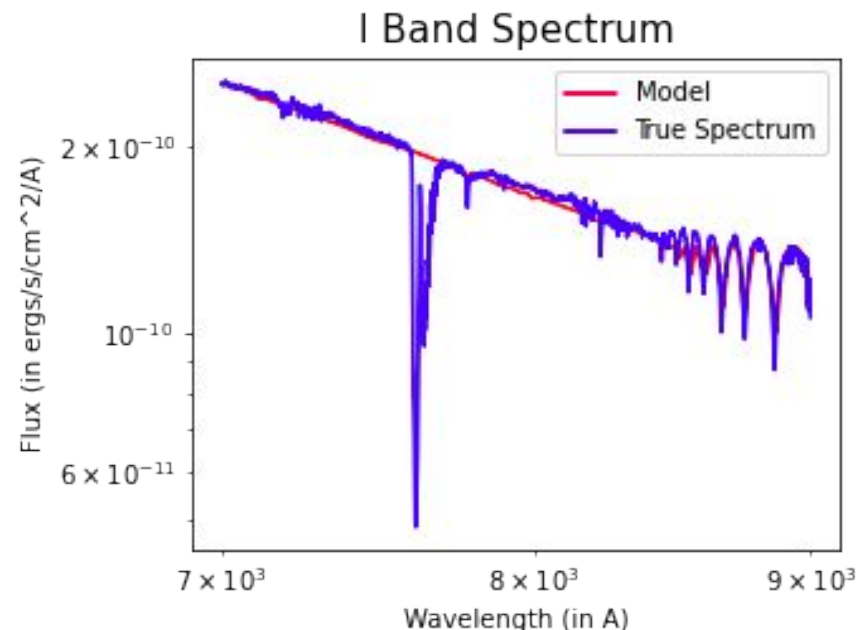
(HD 86986: A1V Star)

Balmer Lines and Balmer Limit

Analysis - Hydrogen spectral series



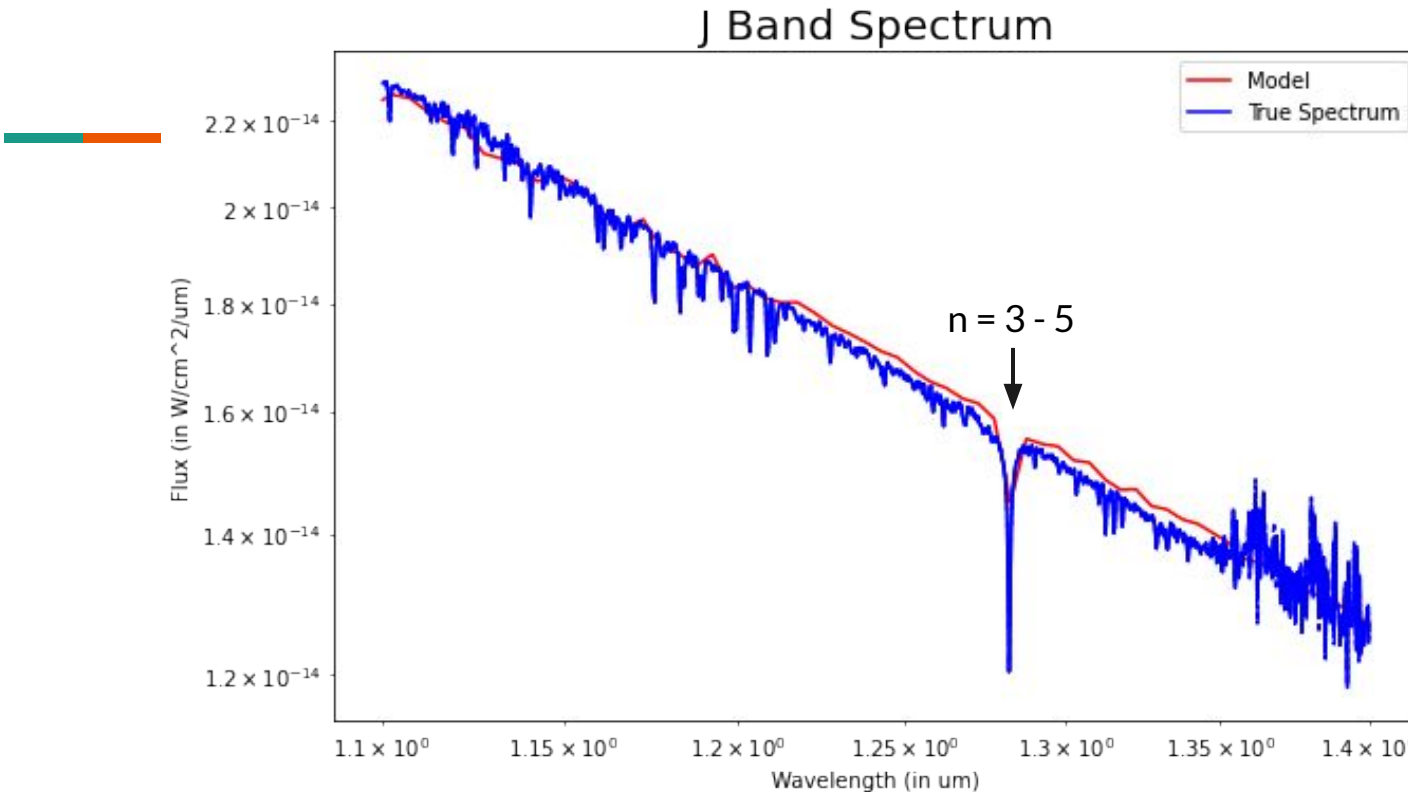
(HD 95418: A1V Star)



(HD 86986: A1V Star)

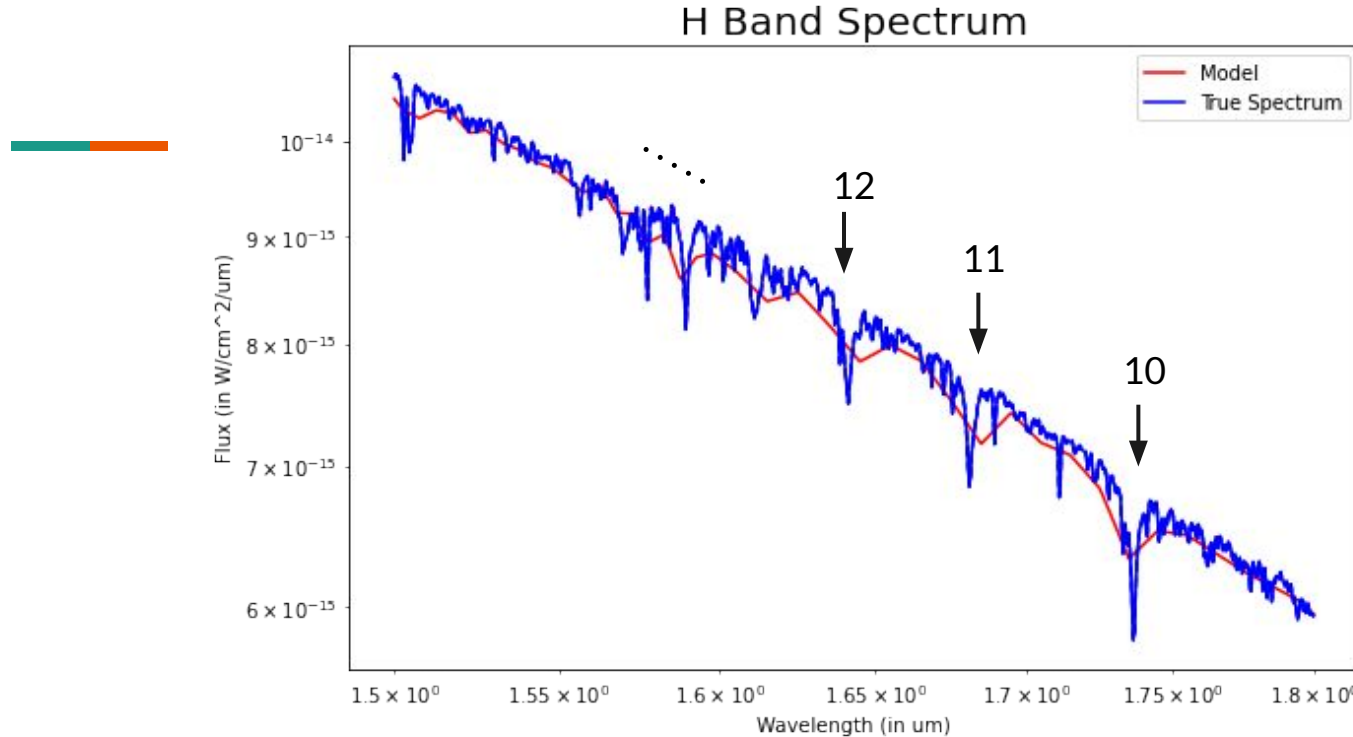
Paschen Lines and Paschen Limit

Analysis - Hydrogen spectral series



HD 126660: F-type Star - an example of model fit to **Paschen series** ($n = 3$ to $n = 5$) in observed flux distribution

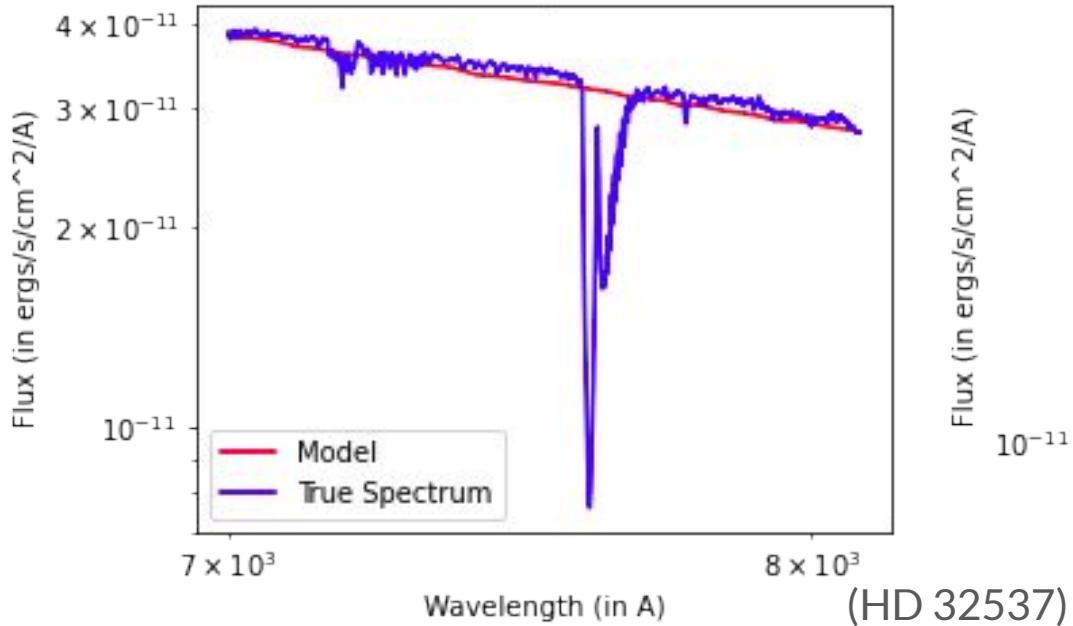
Analysis - Hydrogen spectral series



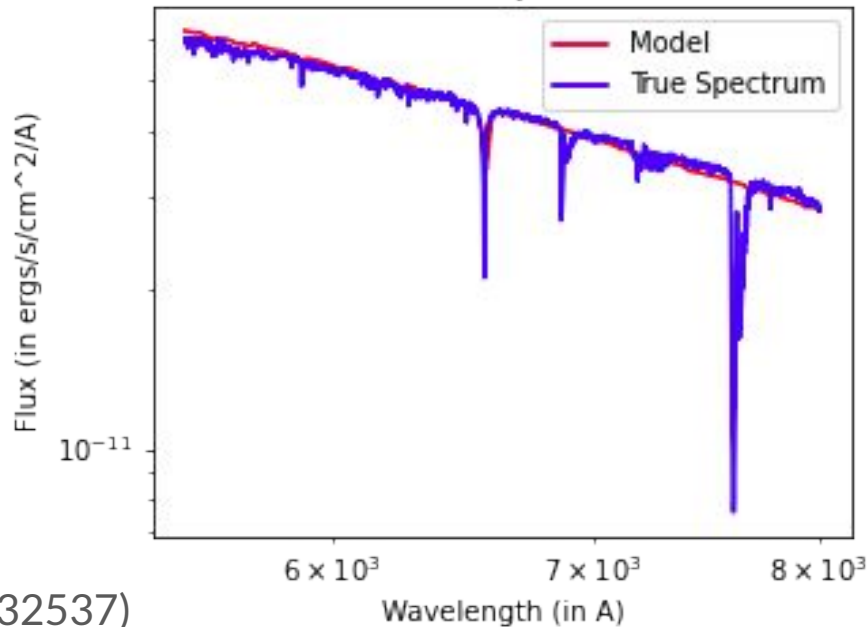
HD 124850: F-type Star - an example of model fit to **Brackett series** in observed flux distribution

Analysis - Atmospheric Absorption

I Band Spectrum



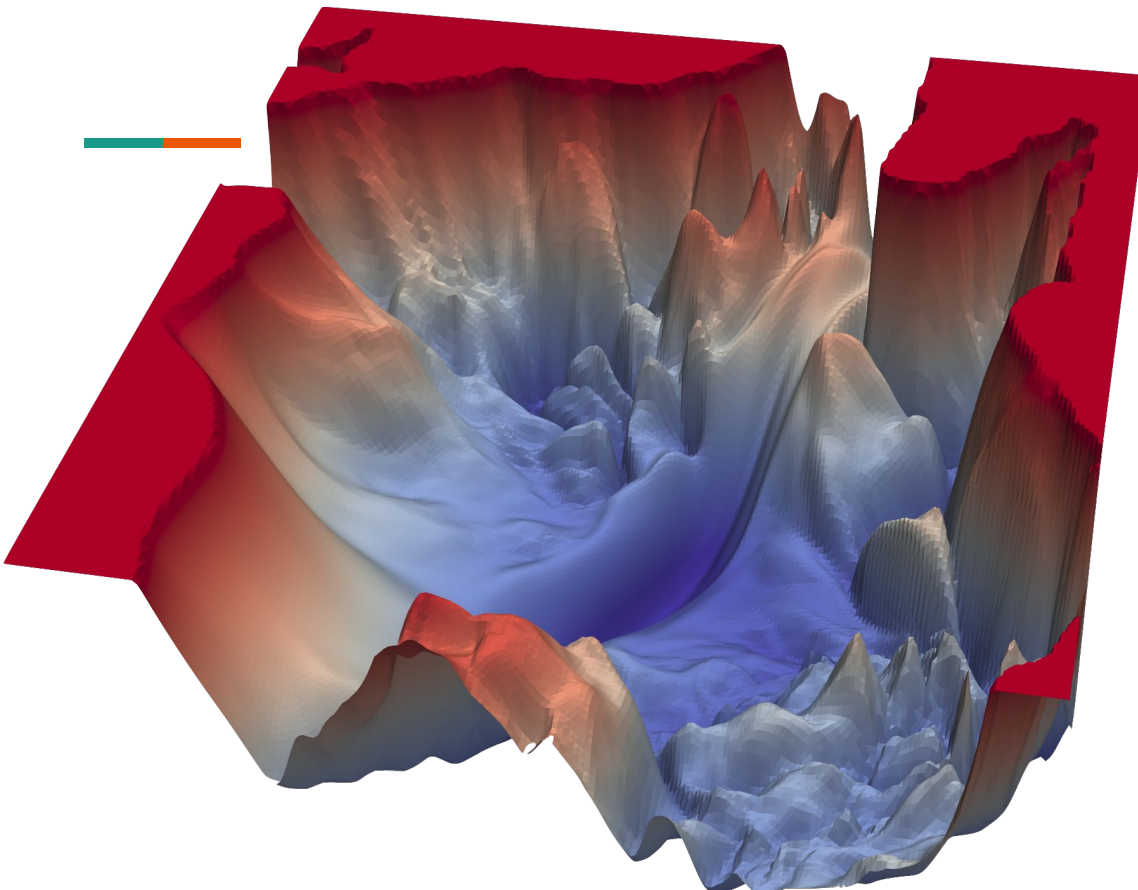
R Band Spectrum



Telluric absorption bands -

1. A Band: 7600-7630 Å (in I Band Spectrum)
2. B Band: 6860-6890 Å (in R Band Spectrum)

Grid-Search - Non-convex optimization



$$a'_j = a_{j,3} - \Delta a_j \left[\frac{\chi_3^2 - \chi_2^2}{\chi_1^2 - 2\chi_2^2 + \chi_3^2} + \frac{1}{2} \right]$$

$$\sigma_j = \Delta a_j \sqrt{2(\chi_1^2 - 2\chi_2^2 + \chi_3^2)^{-1}}$$

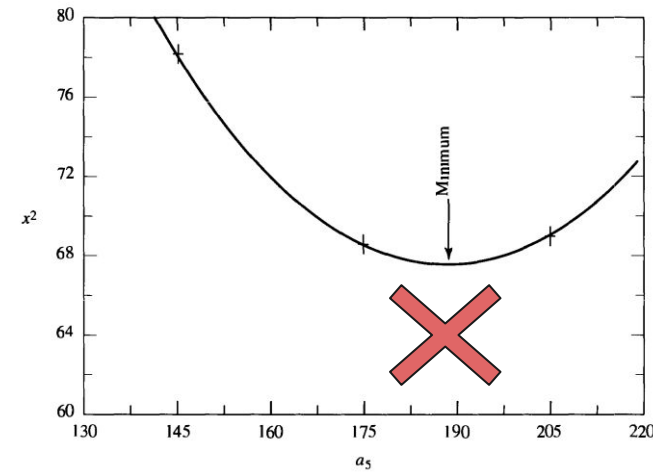


Image Credits: <https://www.cs.umd.edu/~tomg/projects/landscapes/>



Conclusion

Conclusion

From the analysis performed we conclude that

1. Kurucz models can be used to fit synthetic spectra of observed spectra in smaller wavelength range - and still be able to estimate photometric magnitudes in different bands
2. Necessary to constrain the parameter values to obtain physically acceptable models and synthetic SED
3. Grid Search - Non-convex optimization problem
4. Even if [Fe/H] estimate is available - not advisable to use grid search unless the span of search over metallicity is low (~ 0.1 dex)
5. Mass determined using estimate of radius and $\log(g)$ - erroneous.
6. Hyper-giants and dwarfs - not fit by Kurucz models



Future Scope

Future Scope

1. Use of larger dataset to obtain statistical rather than qualitative inferences.
2. Use of Machine Learning based approach to determine stellar properties.
3. Estimation of range of values of grid search parameters from independent approaches to constrain the search to physically acceptable models
 - a. Effective Temperature - Color/Brightness Temperature (T_B might require numerical root finding methods to solve transcendental equation).
 - b. Surface gravity - range from literature
 - c. Metallicity - estimate from equivalent width method.
4. Use of multiple models and taking an ensemble approach for parameter estimation



References

References

1. https://www.aanda.org/articles/aa/full_html/2019/07/aa35723-19/aa35723-19.html#S2
2. <https://pysynphot.readthedocs.io/en/latest/>
3. <http://irtfweb.ifa.hawaii.edu/~spex/IRTF Spectral Library/References files/All.html>
4. J.-F. Le Borgne, et al. “STELIB: a library of stellar spectra at R 2000”, *Astron. Astrophys.* 402:433-442,2003, arXiv:astro-ph/0302334, doi: 10.1051/0004-6361:20030243.
5. Straizys V., Liubertas R. and Valiauga G., Kurucz Model FLux Distributions: A Comparison With Real Stars, *Baltic Astronomy*, vol. 6, 601-636, 1997.
6. Straizys V., Liubertas R. and Valiauga G., Kurucz Model FLux Distributions: A Comparison With Real Stars. II Metal-Deficient Stars, *Baltic Astronomy*, vol. 11, 341-366, 2002.

THANK YOU

QUESTIONS

APPENDIX

Analysis - STELIB Data (BV only)

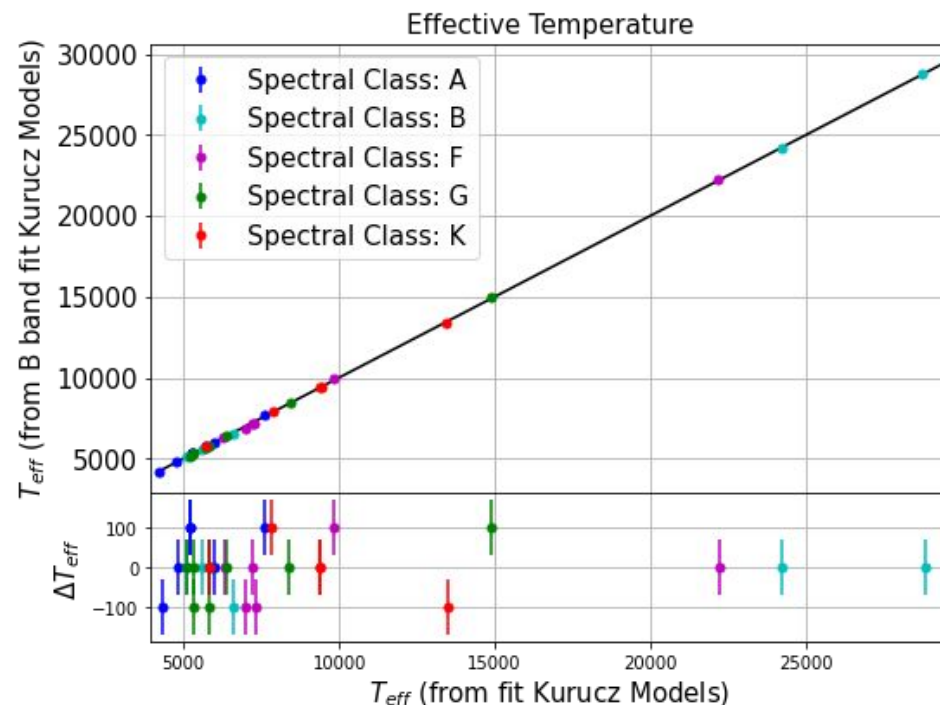


Figure: Comparison of effective temperature determined from B band fit with overall fit

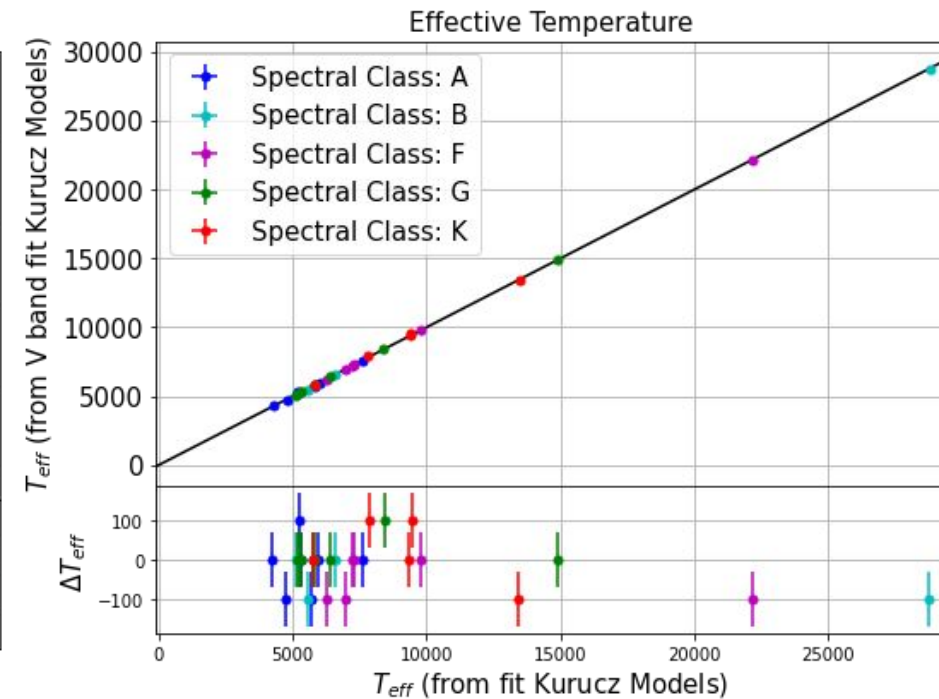


Figure: Comparison of effective temperature determined from V band fit with overall fit

Match between parameters from B/V band fit to overall fit

Analysis - STELIB Data (BV only)

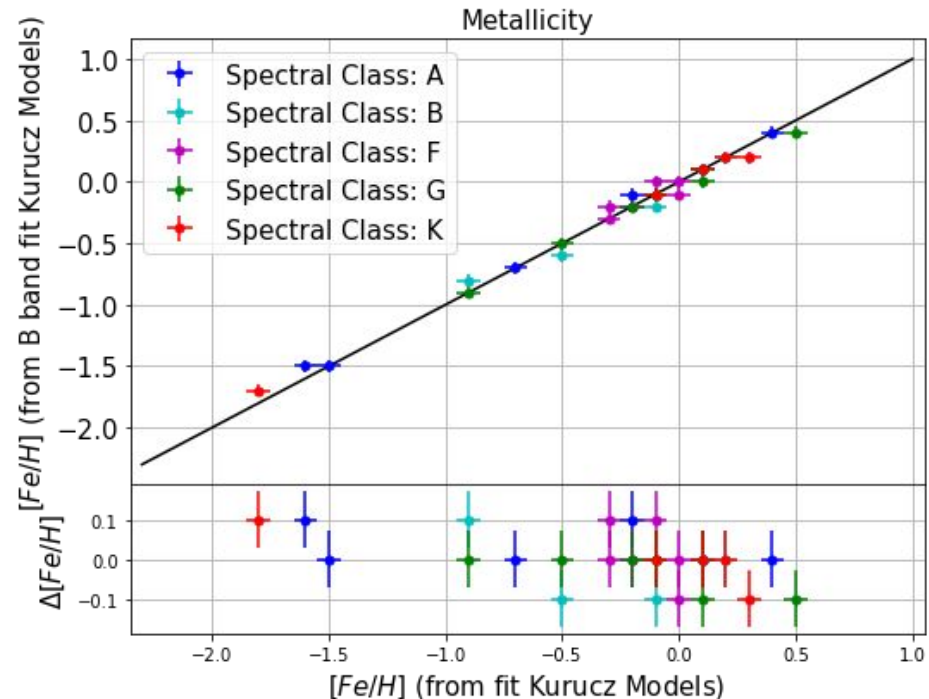


Figure: Comparison of metallicity determined from B band fit with overall fit

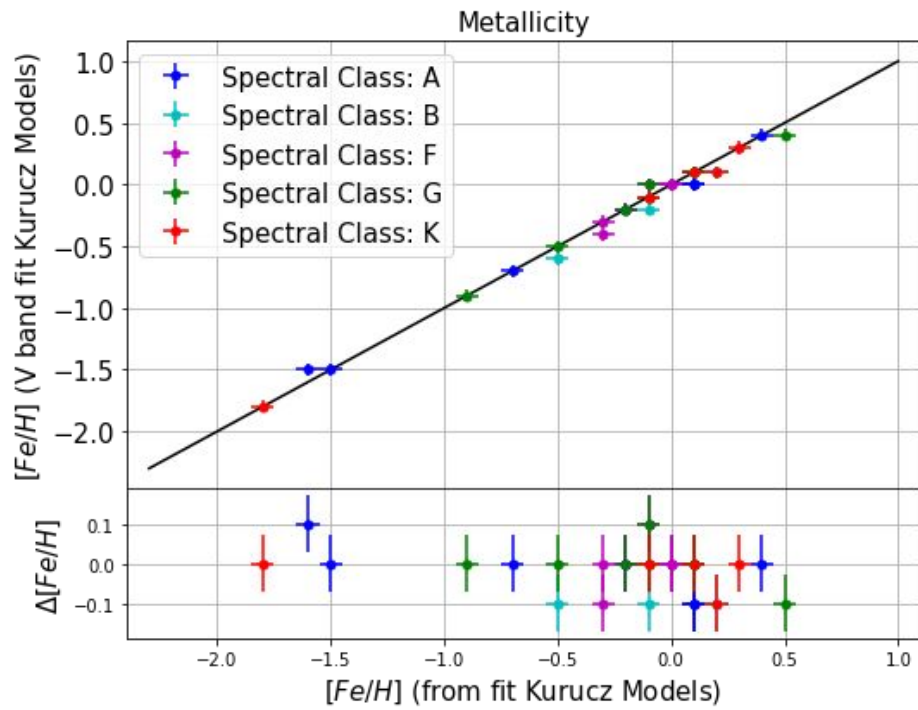


Figure: Comparison of metallicity determined from V band fit with overall fit

Match between parameters from B/V band fit to overall fit

Analysis - STELIB Data (BV only)

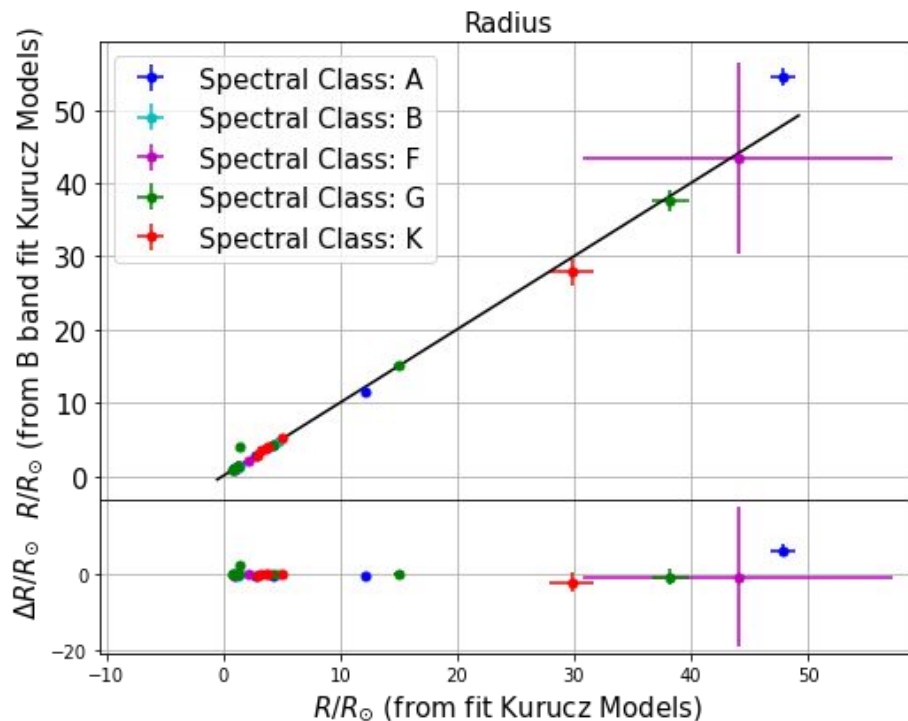


Figure: Comparison of radius determined from B band fit with overall fit

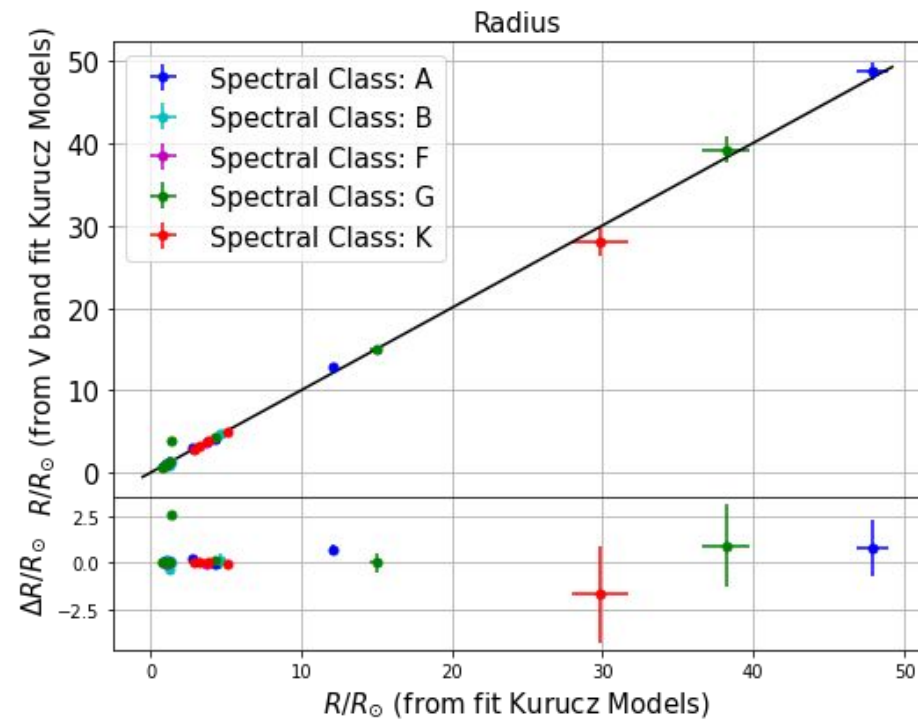
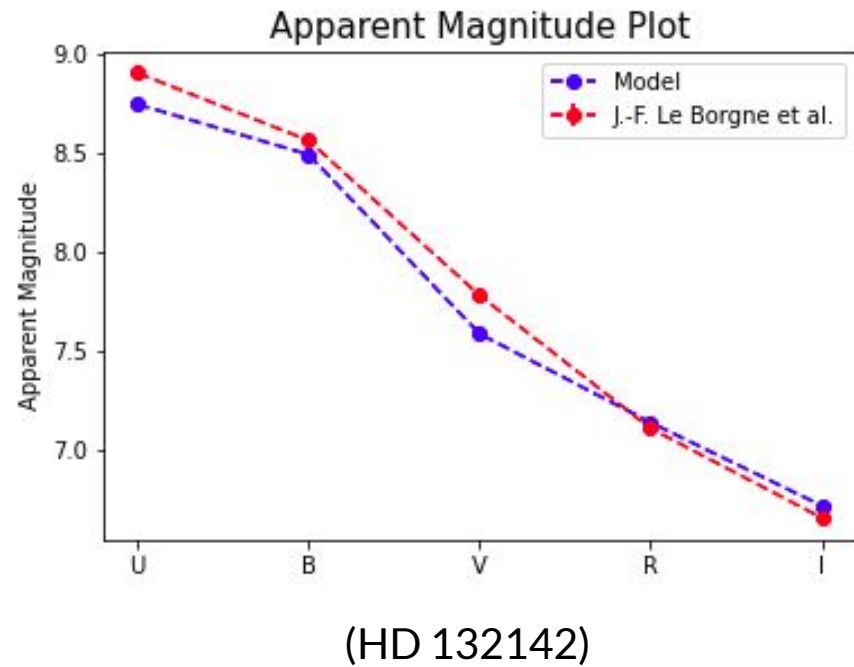
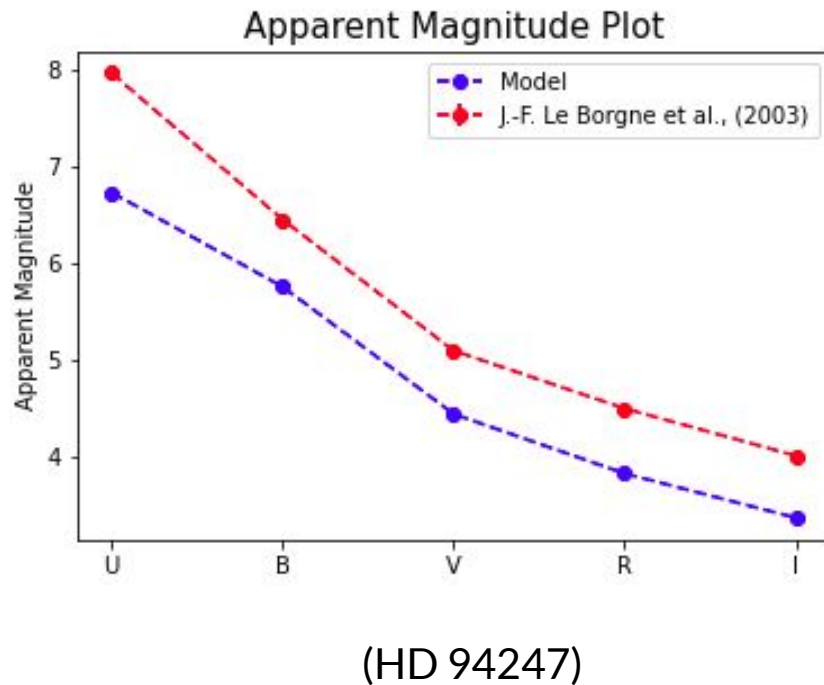


Figure: Comparison of radius determined from V band fit with overall fit

Match between parameters from B/V band fit to overall fit

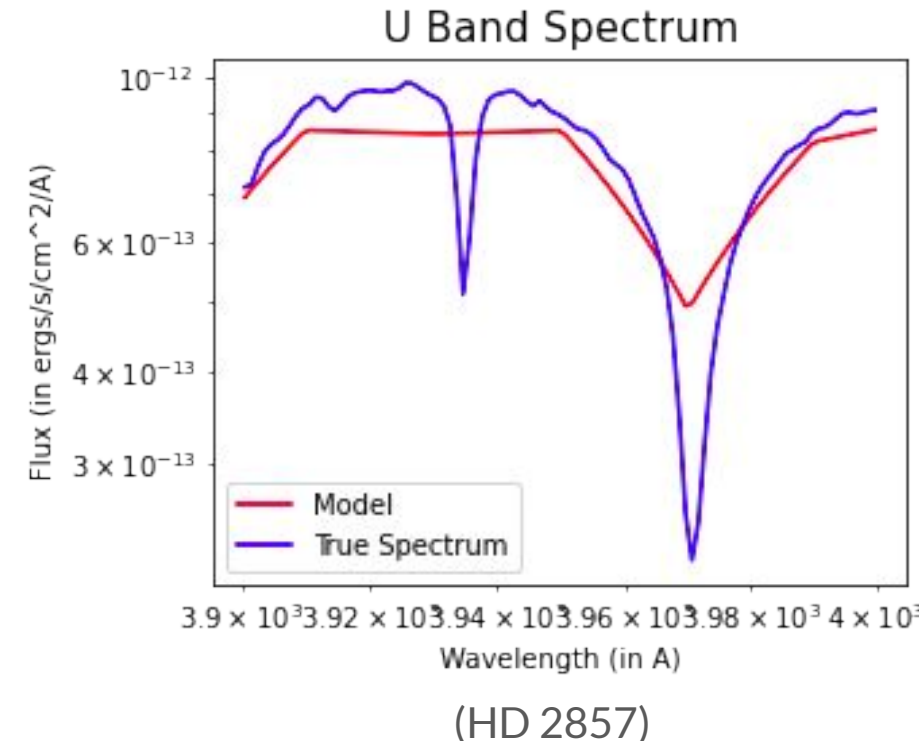
Appendix - Photometry in K-Type stars



Theory

```
TEFF 5777. GRAVITY 4.43770 LTE
TITLE [0.0] VTURB=1.0 KM/SEC L/H=1.25 NOVER NEW ODF
OPACITY IFOP 1 1 1 1 1 1 1 1 1 1 1 1 1 0 1 0 0 0 0 0
CONVECTION ON 1.25 TURBULENCE OFF 0.00 0.00 0.00 0.00
ABUNDANCE SCALE 1.00000 ABUNDANCE CHANGE 1 0.92040 2 0.07834
ABUNDANCE CHANGE 3 -10.94 4 -10.64 5 -9.49 6 -3.52 7 -4.12 8 -3.21
ABUNDANCE CHANGE 9 -7.48 10 -3.96 11 -5.71 12 -4.46 13 -5.57 14 -4.49
ABUNDANCE CHANGE 15 -6.59 16 -4.71 17 -6.54 18 -5.64 19 -6.92 20 -5.68
ABUNDANCE CHANGE 21 -8.87 22 -7.02 23 -8.04 24 -6.37 25 -6.65 26 -4.54
ABUNDANCE CHANGE 27 -7.12 28 -5.79 29 -7.83 30 -7.44 31 -9.16 32 -8.63
ABUNDANCE CHANGE 33 -9.67 34 -8.63 35 -9.41 36 -8.73 37 -9.44 38 -9.07
ABUNDANCE CHANGE 39 -9.80 40 -9.44 41 -10.62 42 -10.12 43 -20.00 44 -10.20
ABUNDANCE CHANGE 45 -10.92 46 -10.35 47 -11.10 48 -10.27 49 -10.38 50 -10.04
ABUNDANCE CHANGE 51 -11.04 52 -9.80 53 -10.53 54 -9.87 55 -10.91 56 -9.91
ABUNDANCE CHANGE 57 -10.87 58 -10.46 59 -11.33 60 -10.54 61 -20.00 62 -11.03
ABUNDANCE CHANGE 63 -11.53 64 -10.92 65 -11.69 66 -10.90 67 -11.78 68 -11.11
ABUNDANCE CHANGE 69 -12.04 70 -10.96 71 -11.98 72 -11.16 73 -12.17 74 -10.93
ABUNDANCE CHANGE 75 -11.76 76 -10.59 77 -10.69 78 -10.24 79 -11.03 80 -10.91
ABUNDANCE CHANGE 81 -11.14 82 -10.09 83 -11.33 84 -20.00 85 -20.00 86 -20.00
ABUNDANCE CHANGE 87 -20.00 88 -20.00 89 -20.00 90 -11.95 91 -20.00 92 -12.54
ABUNDANCE CHANGE 93 -20.00 94 -20.00 95 -20.00 96 -20.00 97 -20.00 98 -20.00
ABUNDANCE CHANGE 99 -20.00
READ DECK6 72 RHOX,T,P,XNE,ABROSS,ACCRAD,VTURB, FLXCNV,VCONV,VELSND
5.85641157E-04 3650.6 1.604E+01 2.691E+09 2.277E-04 4.614E-02 1.000E+05 0.000E+00 0.000E+00 6.696E+05
7.64075733E-04 3679.3 2.093E+01 3.460E+09 2.708E-04 5.246E-02 1.000E+05 0.000E+00 0.000E+00 6.624E+05
9.64357866E-04 3708.1 2.642E+01 4.323E+09 3.215E-04 5.875E-02 1.000E+05 0.000E+00 0.000E+00 6.581E+05
```

Analysis - Atmospheric Absorption



Calcium H and K lines:

1. 3934 Å - Ca II K line - fit in models with high [Fe/H]
2. 3968 Å - Ca II H line (blended with H-epsilon line)

Theory

- b. Opacity Distribution Function: (ATLAS9)
 - a. Spectra - divided into subsections (bins)
 - b. Opacity in a bin - arranged in ascending order
 - c. Wavelength bin - divided into sub-bins (non-uniform width in general)
 - d. Step-function approximation to opacity distribution over bin - constant throughout sub-bin
 - e. Castelli & Kurucz (2004) -
 - use 12 sub-bins
 - f. First 9 sub-bins relative width = 0.1
 - g. 10th, 11th and 12th sub-bin
 - 1/20, 1/30 and 1/60 - finer sampling where opacity is high